THE PENNSYLVANIA STATE UNIVERSITY
SCHREYER HONORS COLLEGE

DEPARTMENT OF GEOSCIENCES

USING BRAZILIAN DISK TESTS TO DEFINE TENSILE STRENGTH OF TWO LITHOLOGIES FROM THE UPPER OATKA CREEK MEMBER OF THE MARCELLUS SHALE

MICHAEL CRONIN
Spring 2011

A thesis
submitted in partial fulfillment
of the requirements
for baccalaureate degrees
in Geosciences and Petroleum and Natural Gas Engineering
with honors in Geosciences.

Reviewed and approved* by the following:

Terry Engelder
Professor of Geosciences
Thesis Supervisor

Peter Heaney
Professor of Geosciences
Honors Adviser

* Signatures are on file in the Schreyer Honors College.

ABSTRACT

The Brazilian Disk test was used to evaluate the Mode I tensile strength of two lithologies (calcareous gray shale and shaley limestone) within the Upper Oatka Creek Member of the Marcellus Shale. Disks with dimensionless thickness ratios between 0.26 and 0.84 were systematically prepared with bedding oriented parallel to the disk face and loaded diametrally until failure at two different strain rates. It was discovered that there was no distinction between loading rates of 0.500mm/min and 1.000mm/min, and that average indirect tensile strengths of the two lithologies were 11.07 MPa (std . dev. = 1.45) and 11.14 MPa (st. dev. = 2.15) respectively. It was also noted that observed tensile strength was not a strong function of dimensionless sample geometry between L/D values of 0.4 and 0.6. Outside of this interval, disk preparation quality control became much more difficult for thinner and thicker samples. While the difference in strength between the two lithologies was not significant, the tensile strength values in the calcareous gray shale were much more consistent and obeyed one peak load (kN) vs. dimensionless sample thickness to diameter ratio trend, while the shaley limestone results displayed several possible trends indicative of a more complex mechanical stratigraphy. The implication is that additional lithofacies are required in limey units to properly describe their mechanical behavior. The future goal of this study is to incorporate current results of this study to existing sequence stratigraphy models in the Appalachian Basin to attempt to develop a predictive geomechanical –stratigraphic model.

TABLE OF CONTENTS

LIST OF FIGURES

LIST OF TABLES

ACKNOWLEDGEMENTS

There are numerous individuals who helped make this thesis project become a reality through the generous donation of their time and energy. First and foremost, I would like to thank Dr. Terry Engelder and the Appalachian Basin Sequence Stratigraphy Group (ABBSG) for giving me the opportunity to use Marcellus Shale core in my thesis project. In particular, Dan Kohl was instrumental in his support on the stratigraphy. Without their support, none of this would have been possible. In addition, I would like to thank the following individuals; Dr. Chris Marone, Dr. Dave Shellman, and Dr. Jamal Rostami for offering me laboratory space to prepare samples and perform my experiments. Furthermore, I want to thank Travis Call and Marco Scuderi for their assistance in core preparation. Finally, I must thank the faculty in the Department of Geosciences and Petroleum Engineering for your tireless commitment to my education.

Chapter 1

Introduction

Hydraulic fracturing is a widely used technique in industry to enhance production of hydrocarbons from low permeability formations by inducing large, high permeability fractures that are subsequently held open by proppants. This technique requires pumping water at high pressure into a reservoir until the formation's break down pressure is achieved, and a fracture can be initiated. This breakdown pressure has been theoretically well described (Hubbert and Willis, 1957) as a function of the in situ stress field and the rock's tensile strength. The Hubbert and Willis relation has been well validated in laboratory and field studies (Haimson and Fairhurst, 1967; Raleigh et al., 1972). However, two critical unknowns required to use the Hubbert and Willis relation are the rock tensile strength and the magnitude of the maximum principal stress. The magnitude and direction of the maximum principal stress may be inferred from a variety of observational and in-situ techniques (Engelder, 1987), but the tensile strength must be determined through laboratory techniques or interpretation of field hydraulic fracture tests (Abou-Sayed and Brechtel, 1978). However, the subsequent validity of tensile strength predictions based on field testing is contingent on the accuracy of the maximum principal stress, which can have large local and regional variations. In addition to tensile strength, another important rock property in fracture mechanics is the fracture toughness, which describes the stresses required for brittle reactivation of an existing crack (Ayatollahi and Aliha, 2008). This property is important because reservoir rocks often feature microcracks and fractures that can be reactivated during hydraulic fracturing.

Unconventional natural gas plays like the Marcellus Shale are being developed solely as a result of advances in hydraulic fracturing techniques. However, current understanding of Marcellus fracture mechanics must be expanded to include the relationship between tensile strength and fracture toughness, similar to studies by other researchers on a Saudi Arabian reservoir (Al-Shayea et al., 2001). In addition, the relationship between laboratory determined values of tensile strength to field hydraulic fracturing predictions for tensile strength must be constrained. Furthermore, variations in these fracture mechanical properties must be studied for different lithologies.

In this study, I propose to use the Brazilian disk method (Hondros, 1959) to indirectly determine the rock tensile strength of two Marcellus Shale lithologies from the fold and thrust belt of the Appalachian Basin. In Brazilian disk testing, a polished disk of rock is loaded along the diameter until a mode I (tensile) crack is created along the axis of loading. The Brazilian test was developed for homogeneous isotropic materials, but it has been used successfully to determine tensile strength in anisotropic rocks that feature transverse isotropy due to bedding or foliations (Chen, Pan, and Amadei, 1998; Claesson and Bohloli, 2002; Li and Aubertin, 2002) (Fig 1-1). In addition, several researchers (Chang, Lee, and Jeon, 2002; Wang et al., 2004;) have modified the original method by using different disk geometries or pre-weakening the sample with notches.

The goal of this study is to replicate a vertical fracture cutting across bedding because this is the most common orientation in field hydraulic fractures, and use of the Hubbert and Willis relation requires this fracture orientation. Brazilian tests on anisotropic bedded materials are typically prepared with bedding perpendicular to the disk face (Chen, Pan, and Amadei, 1998) (Figure 1-1). However, due to difficulties with sample preparation, conventional Brazilian disks with an equivalent desired fracture orientation were prepared with bedding parallel to the disk face (Figure 2-2). Furthermore, I intend to constrain the relationship between

tensile strength and dimensionless geometry (thickness to diameter ratio) in addition to improving current understanding of the role of dimensionless geometry and bedding orientation on observed fracture orientations.

Chapter 2

Methods

1. Experimental Set Up

To create vertical Mode I (tensile) fractures in a bedded material to simulate field hydraulic fractures, two equivalent disk orientations are possible (Fig 2-1C and Fig 2-2). For practical purposes, disks with bedding oriented parallel to disk face were chosen because they were easier to prepare and minimized core disturbance. To conduct the Brazilian Disk tests, an Instron 4202 Room Temperature Load Machine Apparatus was used with a 10kN load cell and flat bearing blocks. To minimize high sample stress concentrations along the sample loading points, a single graphite sheet was placed on the sample top and bottom edges for some samples. Samples with small defects or asperities were oriented such that the defect was perpendicular to the loading axis to minimize the effect of sample heterogeneities. Testing conditions were at atmospheric pressure and room temperature, with a strain rate of 0.500mm/min or 1.000mm/min utilized. and instantaneous load (kN) output to a data logger every 0.5 seconds. Samples were loaded until failure, and the fracture orientation, continuity, mode, and peak load were documented.

The indirect tensile strength of each specimen was determined by the following formula (ASTM D 3967 – 08):

$$\sigma_t = 2P/(\pi LD) \qquad (1)$$

Where:

σ_t = tensile strength (MPa)
P = maximum applied load (N)
L = sample thickness (m)
D = sample diameter (m)

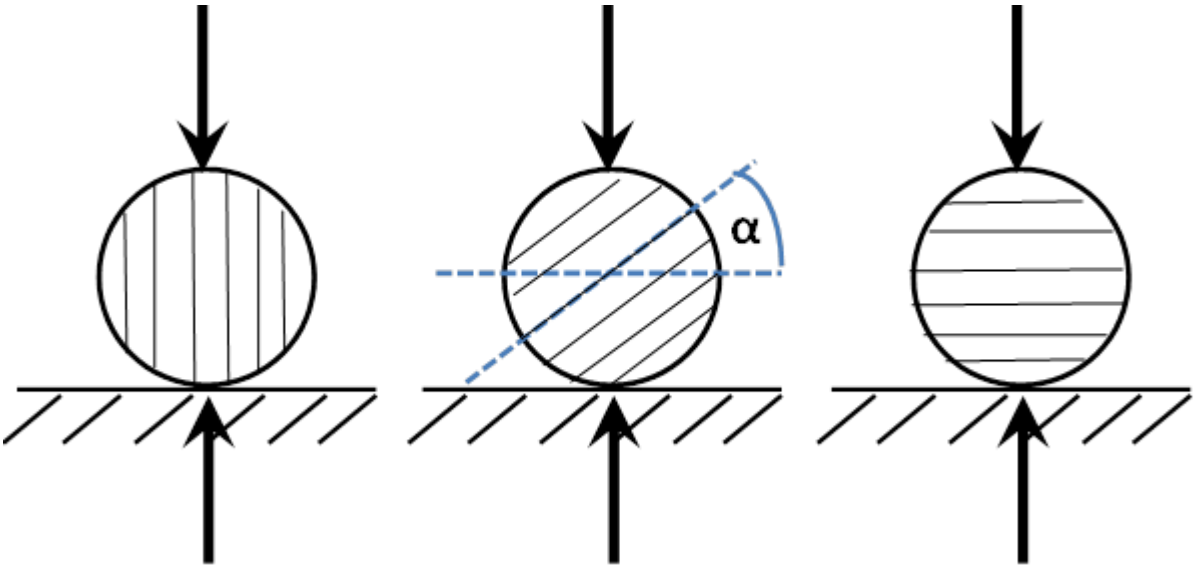

Figure **2-1**: Conventional orientations of anisotropic (bedded) materials during Brazilian Disk tests, where beds are oriented at any arbitrary angle α with respect to the loading direction (B). End member cases are when bedding is parallel or perpendicular to loading, where $\alpha = 0^o$ (A) and α = 0o (C) respectively.

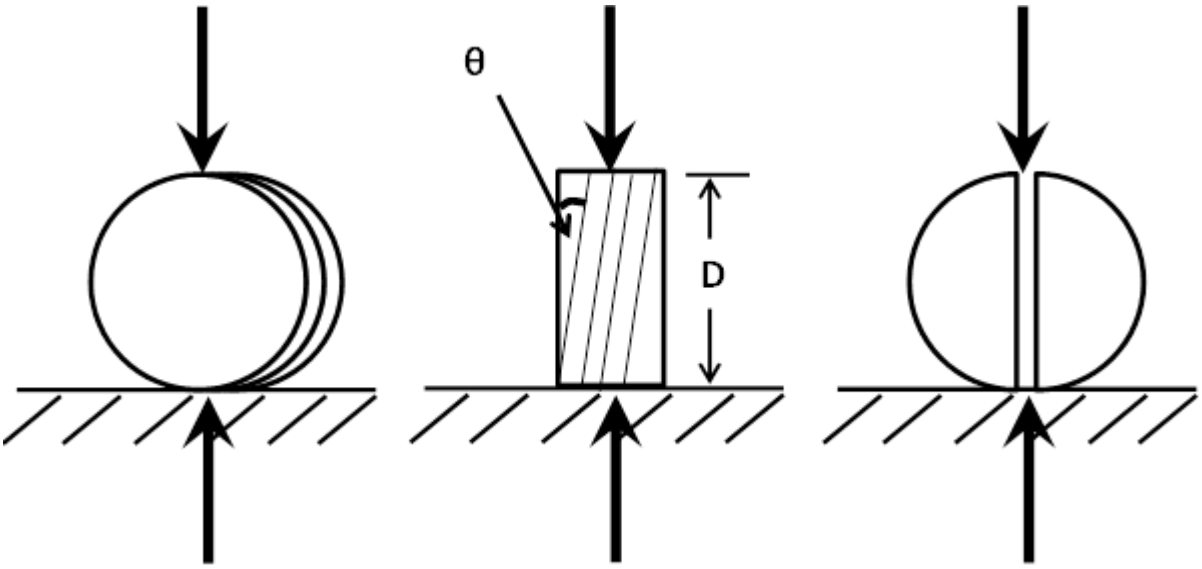

Figure **2-2**: Left, Middle: Definition sketch of Brazilian Disk sample orientation, where θ = apparent difference in degrees between disk face and bedding dip with respect to loading direction. Bedding is ideally parallel to the disk face ($\theta = 0^o$). Right: Ideal "half moon" fracture orientation for valid results.

2. Lithology of Samples and Disk Preparation.

A calcareous gray shale (Fig **2-2a)** and a shaley limestone (**2-2b)** were selected from a 2" diameter core acquired from the Oatka Creek Member of the Marcellus Shale occurring in the Valley and Ridge Province of the Appalachian Basin. Core data was acquired from Well SGL 252 2010 (Lat: 41.136019^{o} Long: -76.955857^{o}) (Figure 2-3a,b). Average gamma ray log values for the calcareous gray shale and the shaley limestone were approximately 210 and 180 respectively.

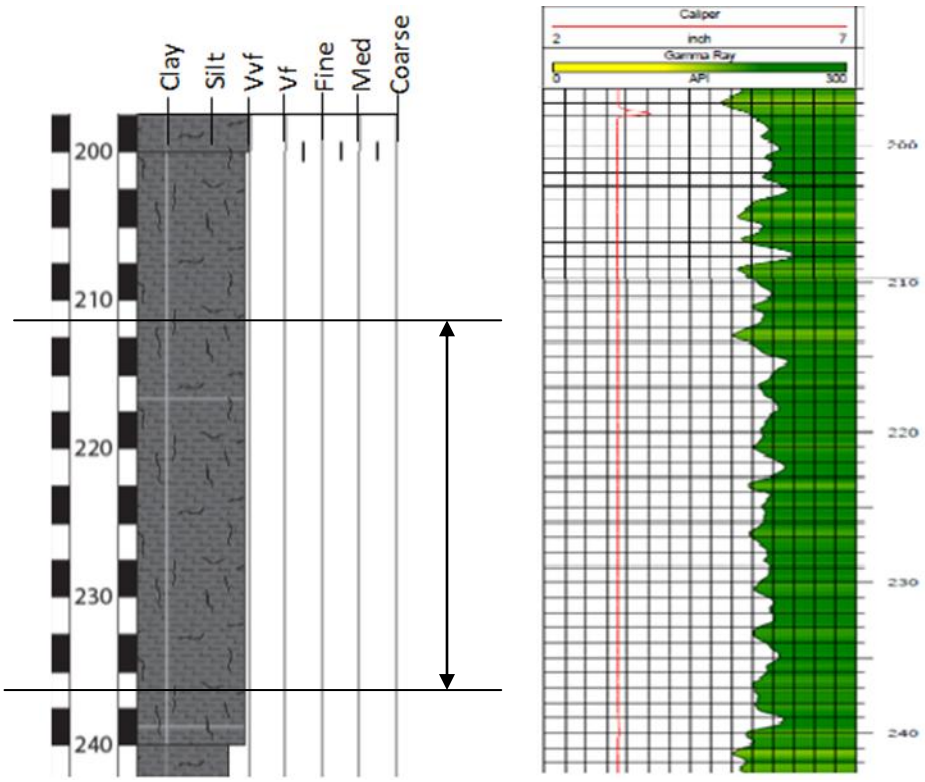

Figure **2-2a**: Core graphic log side by side with gamma ray log of calcareous gray shale lithology of the Oatka Creek Member in Well SGL 252 2010. Lithology of interest sampled between 212 ft KB and 236 ft KB. Graphic log modified after Dan Kohl 2011. Gamma ray scale 0 (yellow) to 300 (green) API Gamma Ray units.

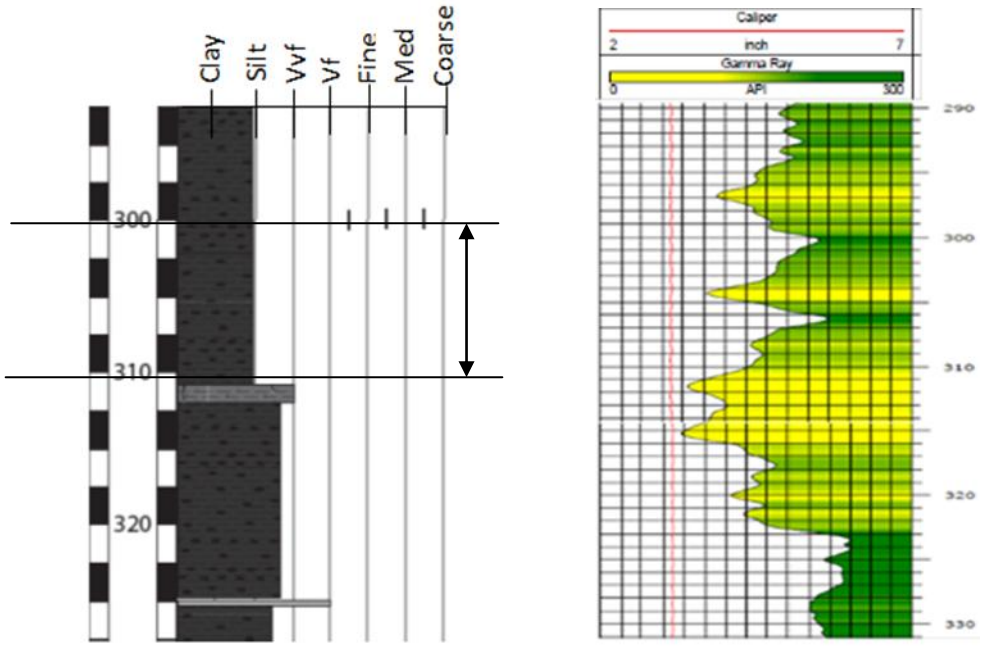

Figure **2-2b**: Core graphic log side by side with gamma ray log of shaley limestone lithology of the Oatka Creek Member in Well SGL 252 2010. Lithology of interest sampled between 300 ft KB and 310 ft KB. Graphic log modified after Dan Kohl 2011. Gamma ray scale 0 (yellow) to 300 (green) API Gamma Ray units.

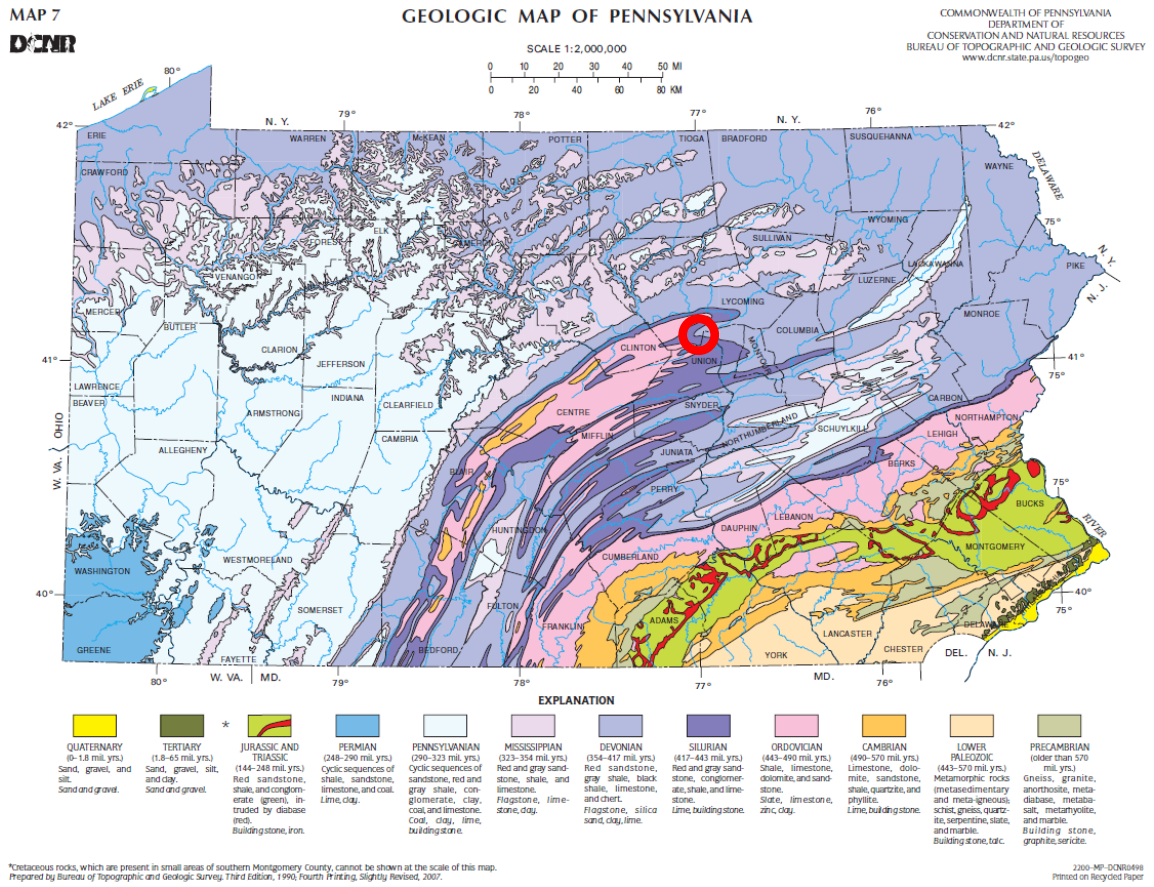

Figure **2-3a**: Geologic map of Pennsylvania, with approximate location of SGL 252 2010 Well depicted in red. Modified after PA Department of Conservation and Natural Resources survey, 2007.

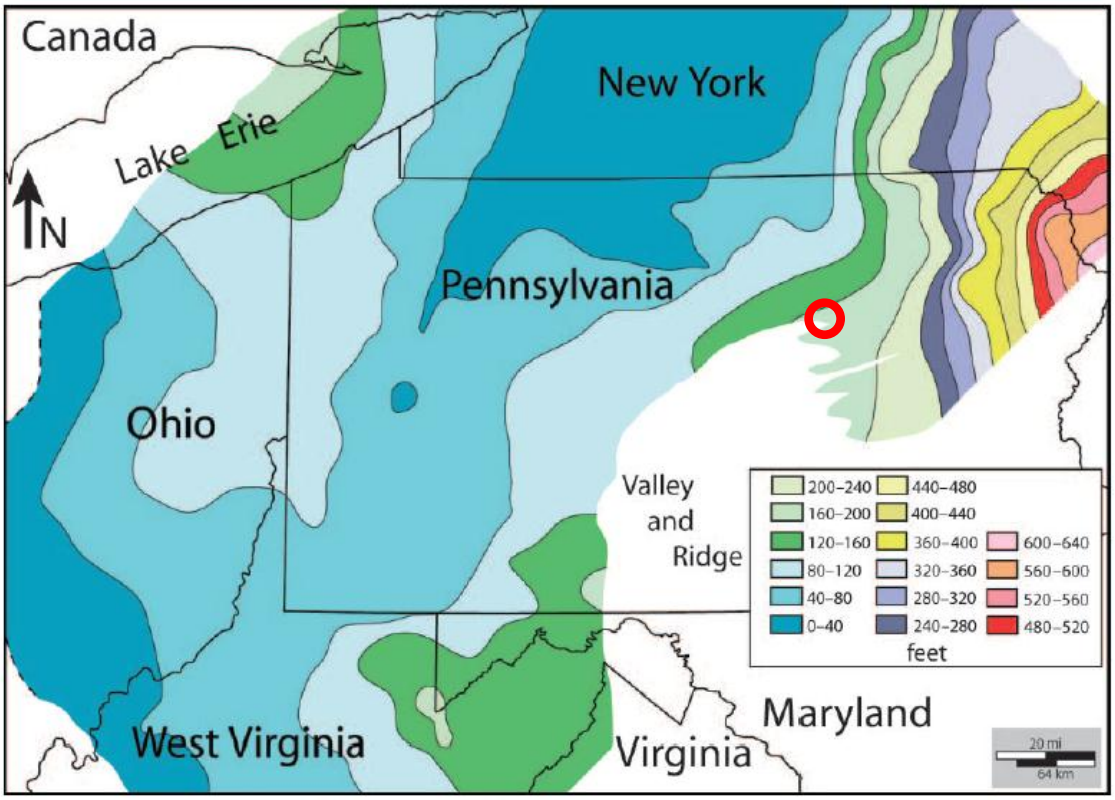

Figure 12. Isochore map of the Oatka Creek Member. The dashed isochore represents the mapped zero line of the Oatka Creek Member; elsewhere, contouring is limited by a lack of data. Isochore lines were not traced into the valley and ridge because of sparse data and structural complexities.

Figure **2-3b**: Isocore map of the Oatka Creek Member of the Marcellus Shale with approximate location of SGL 252 2010 Well depicted in red. Well drilled in the Valley and Ridge Province of the Appalachian Basin. Modified after Lash and Engelder, 2011.

3. Sample Preparation

To minimize localized core heterogeneity, both lithologies were vertically sampled over their respective intervals of occurrence, with care taken to avoid calcite deposits, faults, pyrite deposits, and other structural defects. Due to the 15 – 25^{o} inclination of bedding with respect to the core drilling direction, a series of specialized PVC jackets were used to orient the 2” core and apply a confining stress to minimize failures along bedding while a 1” diameter core was redrilled

perpendicular to bedding from the host core. The samples were drilled using water to cool and lubricate the core barrel.

For use in Brazilian Disk testing, the recommended dimensionless thickness to diameter ratio is 0.2 to 0.75 (ASTM D 3967 – 08). In this investigation, 57 disks with dimensionless thickness to radius ratios between 0.25 and 0.84 were prepared (N gray shale = 22, N shaley limestone = 35). The redrilled core was cut parallel to bedding (perpendicular to core axis) using a laboratory sliding table saw in increments to achieve the approximate desired dimensionless thickness to diameter ratio. A circular sander was then used to correct major asperities and flaws and to reduce sample thickness to achieve the target ratio. When necessary, fine sand paper was used to apply a final polish to disk faces. A digital micrometer was subsequently used to record disk dimensions (diameter and thickness) following ASTM recommendations (ASTM D 3967 – 08).

Chapter 3

Experimental Data

The experimental results section is divided into two sections. The first concerns the physical test results, and includes the load curves and calculated tensile strength values. The second section concerns generalized experimental observations of the fractures generated during testing.

1. Physical Tests

A. **Load Curves**

A family of load curves (kN) vs time (sec) was generated for each lithology by plotting all of the load curves for samples exhibiting Mode I behavior without significant failure along bedding failure (Fig 3-1a,b). In addition, a similar family of load curves was plotted for failures along bedding (Fig 3-2a,b).

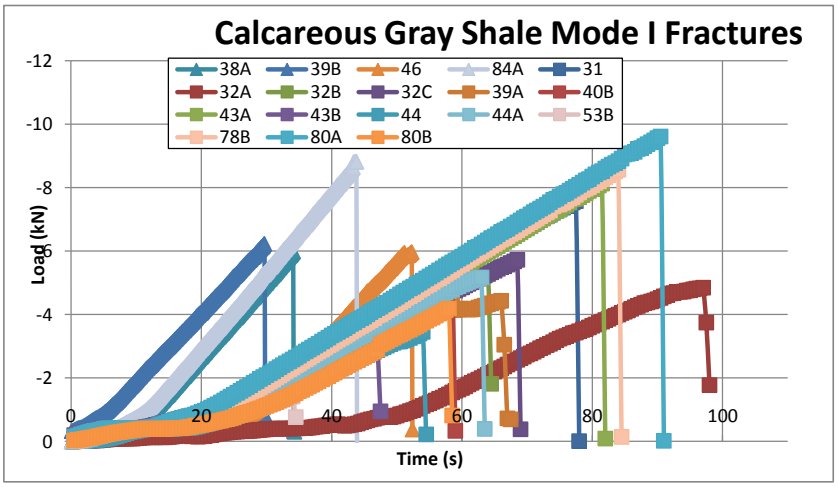

Fig **3-1a**: Plot of loading profiles (kN) vs. time (sec) for all calcareous gray shale samples exhibiting vertical Mode I fractures without significant failure along bedding. N = 18. Steeper loading curves represent load rate of 1.000mm/min. Shallower curves represent 0.500mm/min loading rate.

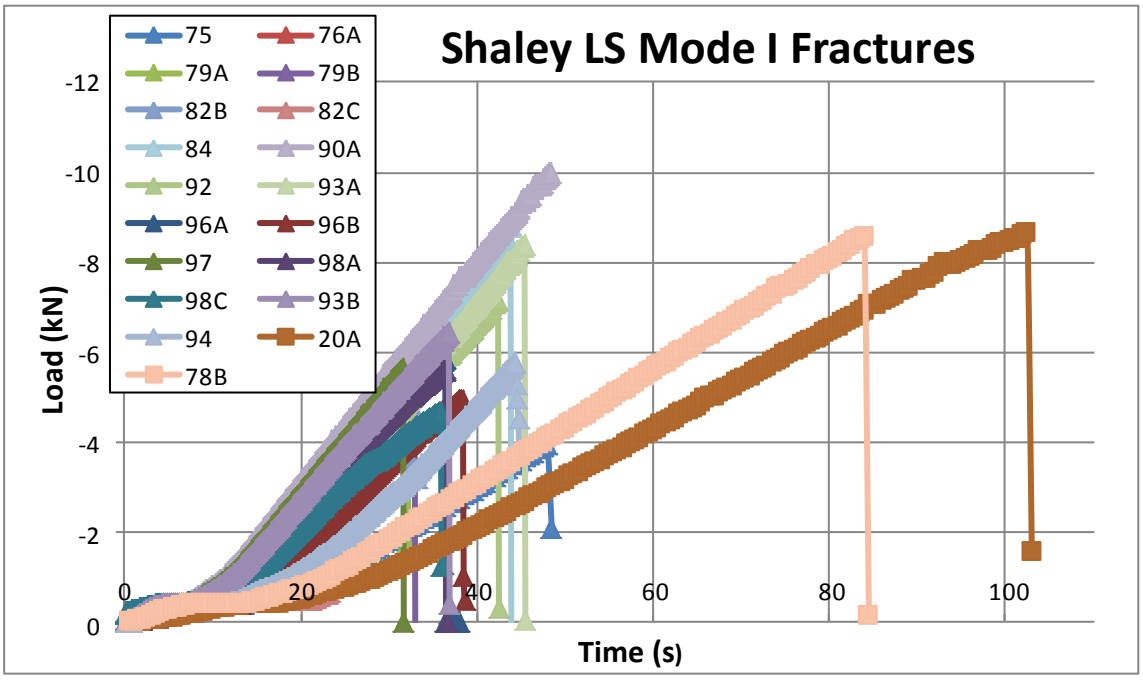

Fig **3-1b**: Plot of loading profiles (kN) vs. time (sec) for all shaley limestone samples exhibiting vertical Mode I fractures without significant failure along bedding. N = 19. Steeper loading curves (triangle legend symbol) represent load rate of 1.000mm/min. Shallower curves (square legend symbol) represent 0.500mm/min loading rate.

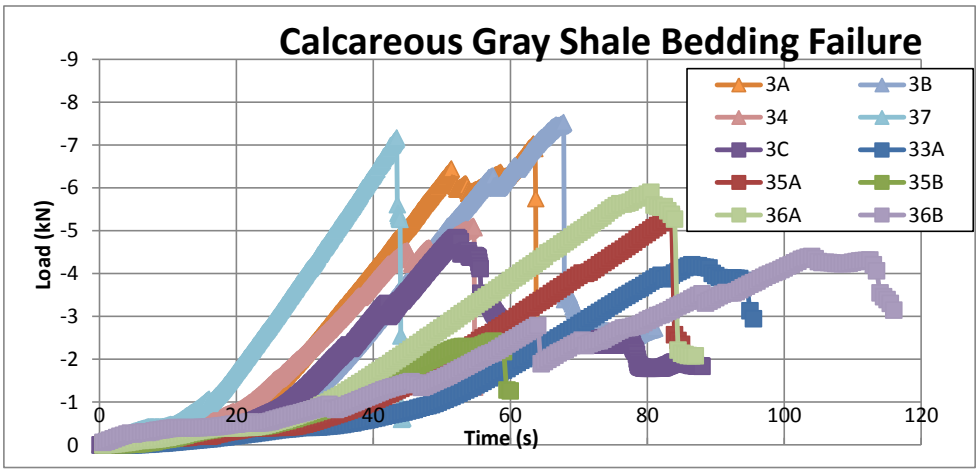

Fig **3-2a**: Plot of loading profiles (kN) vs. time (sec) for all calcareous gray shale samples exhibiting failure along bedding. N = 10. Steeper loading curves (triangle legend symbol)

represent load rate of 1.000mm/min. Shallower curves (square legend symbol) represent 0.500mm/min loading rate.

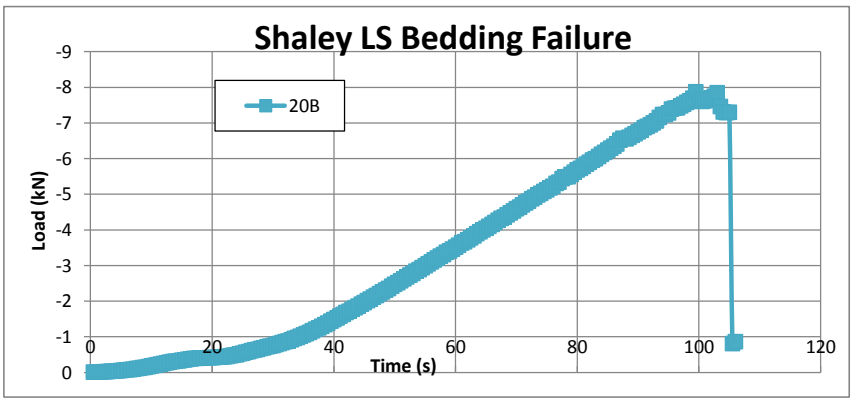

Fig **3-2b**: Plot of loading profiles (kN) vs. time (sec) for all shaley limestone samples exhibiting failure along bedding. N = 1. Sample loaded with 0.500mm/min loading rate.

B. Strength Data

The instantaneous maximum peak load values (kN) recorded prior to sample failure were plotted versus the dimensionless sample thickness to diameter (L/D) ratio for each lithology (Fig 3-3a). In addition, the indirect tensile strength (MPa) predicted by Equation (1) for all samples is plotted against sample dimensionless thickness to diameter ratio (Fig 3-3b). To filter results, similar plots were constructed using only perfect vertical Mode I fractures (Fig 3-5a) that yielded two "half moon" hemispheres with no internal failure on beds and only one primary failure strand (Figure 3-4a, b). The justification for filtering results in this manner is that the previously described "half moon" failure configuration is the only one where the conditions of applicability for Equation (1) are fully met. Experimental data collected for these ideal tests is included in this section (Table 3-1), with all experimental data collected contained in the Appendix.

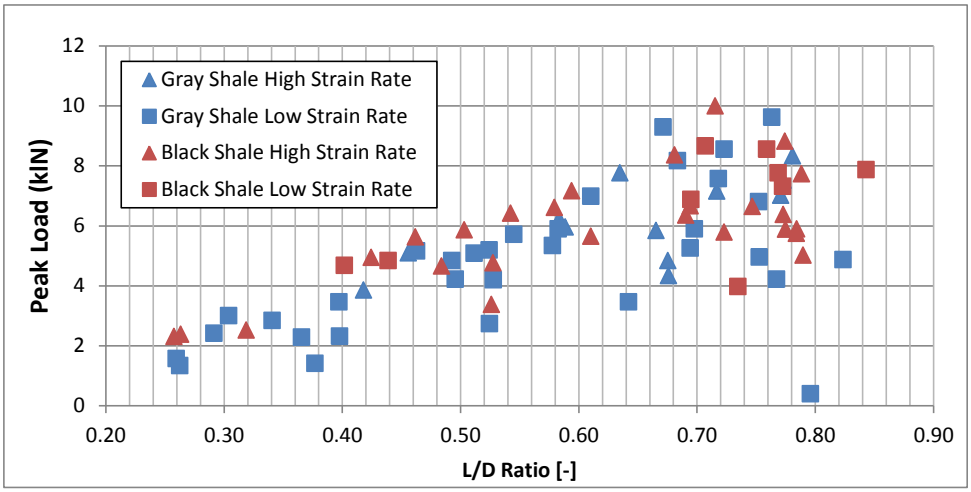

Figure **3-3a:** Peak load (kN) observed during diametral loading vs dimensionless thickness to diameter ratio for all samples. Calcareous gray shale in blue, with shaley limestone in red. Erroneous data point at 0.8 L/D broke during first few seconds of loading and was likely broken during handling. N = 82.

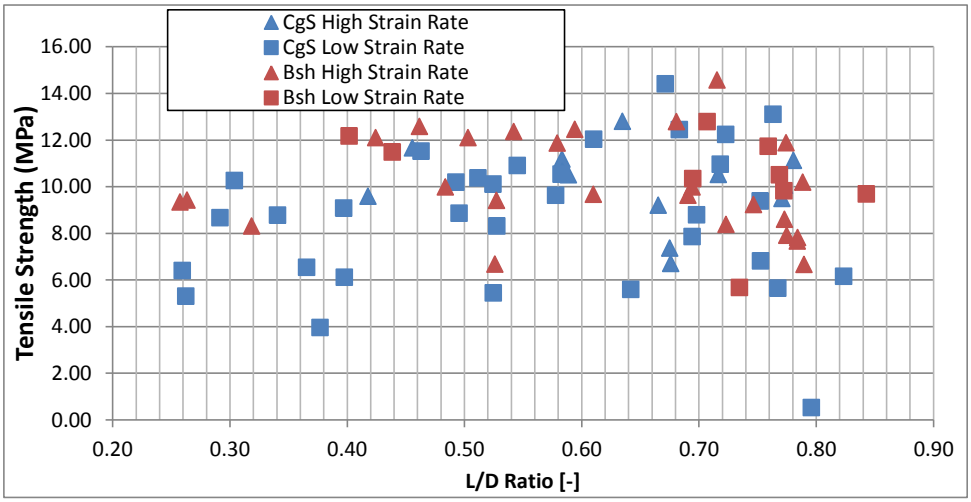

Figure **3-3b**: Indirect tensile stress (MPa) observed during diametral loading vs dimensionless thickness to diameter ratio for all samples. Calcareous gray shale in blue, with shaley limestone

in red. Erroneous data point at 0.8 L/D broke during first few seconds of loading and was likely broken during handling. N= 82.

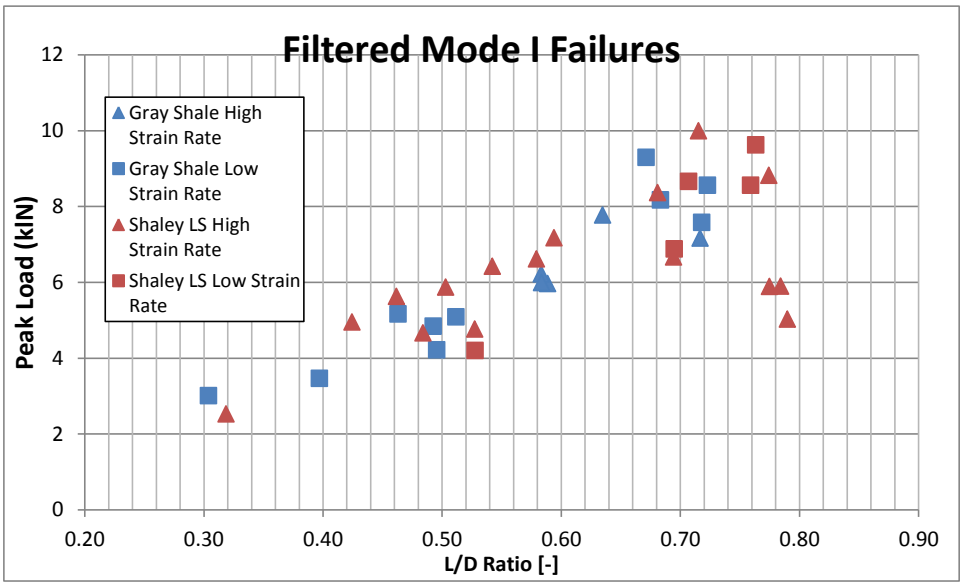

Figure **3-4a:** Peak load (kN) observed during diametral loading vs dimensionless thickness to diameter ratio for all samples failing in the ideal "half moon"manner. Calcareous gray shale in blue, with shaley limestone in red. Triangular data points indicate a strain rate of 1.000mm/min, square data points a strain rate of 0.500mm/min. N = 36.

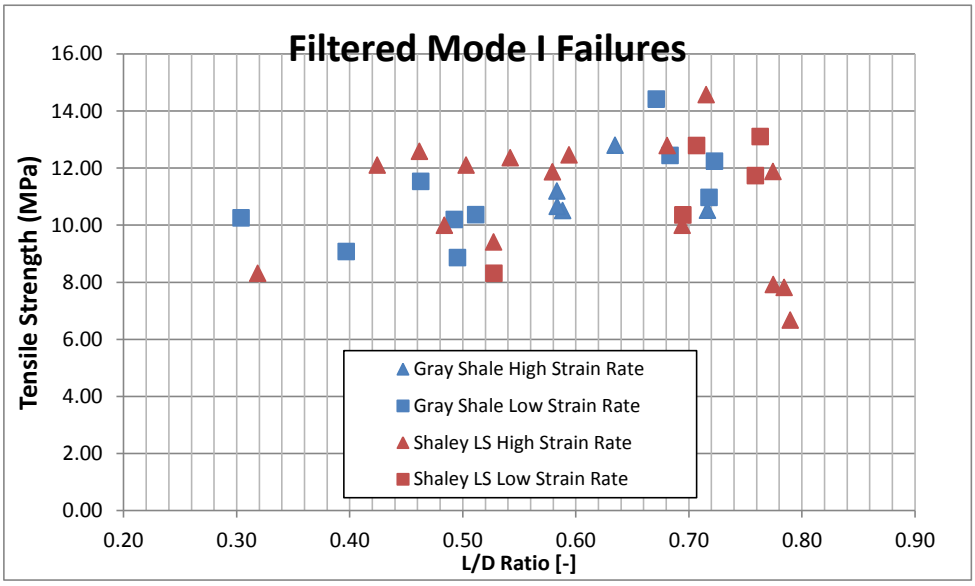

Figure **3-4b**: Indirect tensile stress (MPa) observed during diametral loading vs dimensionless thickness to diameter ratio for samples failing in the ideal "half moon"manner. Calcareous gray shale in blue, with shaley limestone in red. Triangular data points indicate a strain rate of 1.000mm/min, square data points a strain rate of 0.500mm/min. N = 36.

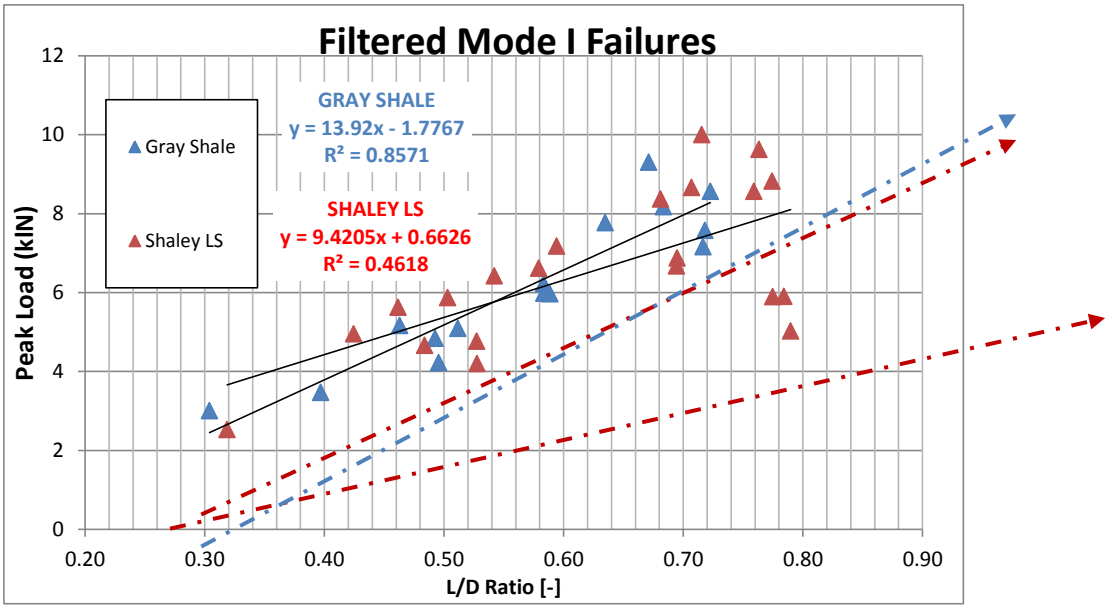

Fig **3-4c**: Linear best fit correlations through plot of peak load (kN) vs L/D for filtered Mode I failures observed in the calcareous gray shale (blue) and the shaley limestone (red). Dotted lines referred to possible strength trends. Solid black lines are best fit lines.

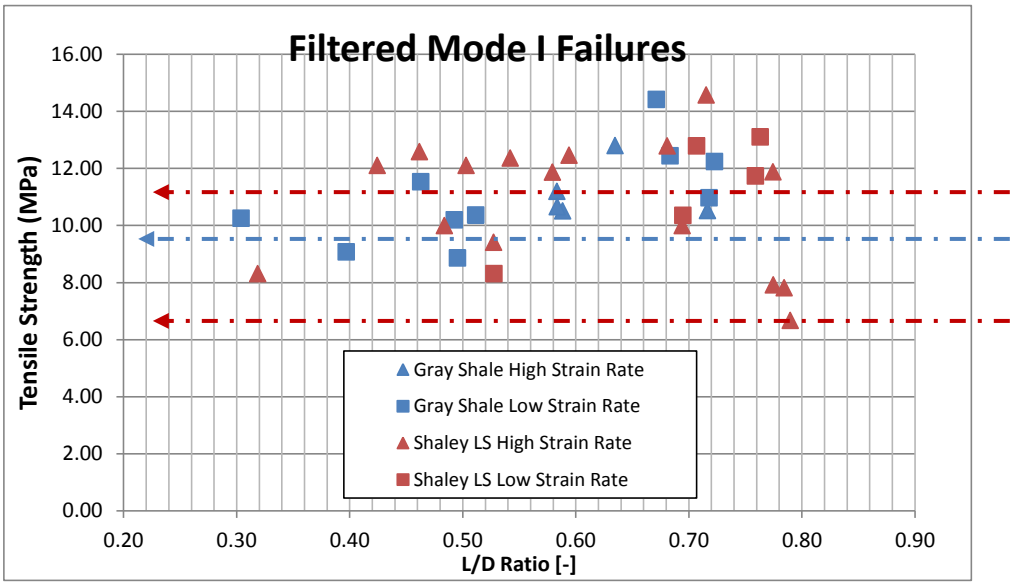

Fig **3-4d**: Linear best fit correlations through plot of tensile strength(MPa) vs L/D for filtered Mode I failures observed in the calcareous gray shale (blue) and the shaley limestone (red). Dotted lines correspond to inferred trends.

Table **3-1**: Summary Table of Ideal ("Half-moon") Mode I vertical fractures and similar quality Mode I fractures. Upper table corresponds to the calcareous gray shale. Lower table corresponds to the shaley limestone.

Strain Rate High = 1.0mm/min Low =0.500mm/min	Sample Group	Run #	Sample Group Depth (ft KB)	Average Diameter, D (mm)	Tensile Strength (Mpa)	Results: (I, M, FB, T)	Comments	Lithology (Courtesy of Dan Kohl)
Low	31	1	232.167	24.75	10.97	I	Perfect Mode I.	CGSh
Low	32	1	233	24.77	10.20	I, O	Bending Vertical Mode I fracture. Vertical in center on front, curved on edge in back.	CGSh
High	37	1	230	24.60	10.52	M, O	Small bed crack at 2kN, bed failure, then Mode I at peak.	CGSh
High	38	1	229.917	24.76	10.66	I	Catastrophic Mode I	CGSh
Low	38	2	229.75	24.82	12.24	O	Mode I, two strand failure. Internal bisection along beds.	CGSh
High	39	2	229.667	24.64	11.19	I, M	Bedding failure, with internal Mode I	CGSh
Low	40	0	217.833	24.74	14.42	I, O	Catastrophic Mode I. Two strand failure.	CGSh
Low	40	2	227.583	24.73	10.37	I, O	Two strand perfect Mode I.	CGSh
High	41	1	217.833	24.67	12.81	I, O	Multi strand Mode I.	CGSh
Low	43	1	227.25	24.74	12.45	I	Mode I Failure	CGSh
Low	43	2	227.25	24.80	10.26	I	Mode I Failure.	CGSh
Low	44	1	210.75	24.83	11.53	I	Perfect complete Mode I.	CGSh
Low	44	2	210.75	24.75	9.08	I	Mode I microcrack at loading tip, then sudden Mode I.	CGSh
High	46	1	229.5	24.79	10.51	I	Catastrophic Mode I	CGSh
Low	53	1	218	24.75	8.86	I	Small vertical fracture started at load block, then propogated mode I	CGSh

AVERAGE TENSILE STRENGTH (Mpa)	11.07
STD DEVIATION	1.44

Strain Rate High = 1.0mm/min Low =0.500mm/min	Sample Group	Run #	Sample Group Depth (ft KB)	Average Diameter, D (mm)	Tensile Strength (Mpa)	Results: (I, M, FB, T)	Comments	Lithology (Courtesy of Dan Kohl)
Low	20	1	302.5	24.69	12.80	I	Perfect Break, Vertical Fracture Straight Through	ShLS
High	76	1	308.5	24.74	10.00	I	Mode I	ShLS
High	76	2	308.5	24.74	9.41	I, O	Offcenter curved Mode I	ShLS
Low	78	1	303	24.68	10.35	I	Mode I Failure	ShLS
Low	78	2	303	24.74	11.74	I	Double Strand Mode I with Island	ShLS
High	79	1	306	24.76	7.82	I	Mode I.	ShLS
High	79	2	306	24.73	7.92	I	Catastrophic Mode I. No bed failures	ShLS
Low	80	1	307.667	24.75	13.11	I	Catastrophic Mode I, dual strand.	ShLS
Low	80	2	307.667	24.70	8.31	I	Mode I	ShLS
High	82	2	308	24.66	6.67	I	Mode I, no bed failure	ShLS
High	82	3	308	24.67	8.31	I	Clean Mode I	ShLS
High	84	1	300.25	24.71	11.88	I	Mode I with multiple vertical strands.	ShLS
High	90	1	301.3	24.70	14.58	I	Mode I half moon failure with Island.	ShLS
High	92	1	301.167	24.84	12.47	I	Half Moon Mode I.	ShLS
High	93	1	303	24.73	12.79	I	Mode I with island. One half had bed failure.	ShLS
High	93	2	303	24.70	12.37	I	Mode I, w/ two strands. Almost perfect half moon fail.	ShLS
High	95	1	309.833	24.76	11.87	I	Splitting Mode I (Split Front, Single strand Back).	ShLS
High	96	1	306.75	24.78	12.10	I	Perfect Mode I half moon failure.	ShLS
High	96	2	306.75	24.78	12.11	I	Mode I, multi strand half moon.	ShLS
High	98	1	306	24.84	12.59	I	Perfect Mode I half moon failure.	ShLS
High	98	3	306	24.79	10.00	I	Half Moon Mode I.	ShLS
		AVERAGE TENSILE STRENGTH (Mpa)			11.14			
		STD DEVIATION			2.31			

2. Observation of Fractures

Included in this section is a series of schematics depicting the general categories of fractures observed along with representative photographs taken of real fractures produced in the Brazilian disks tested in this study.

A. Conventional Fractures

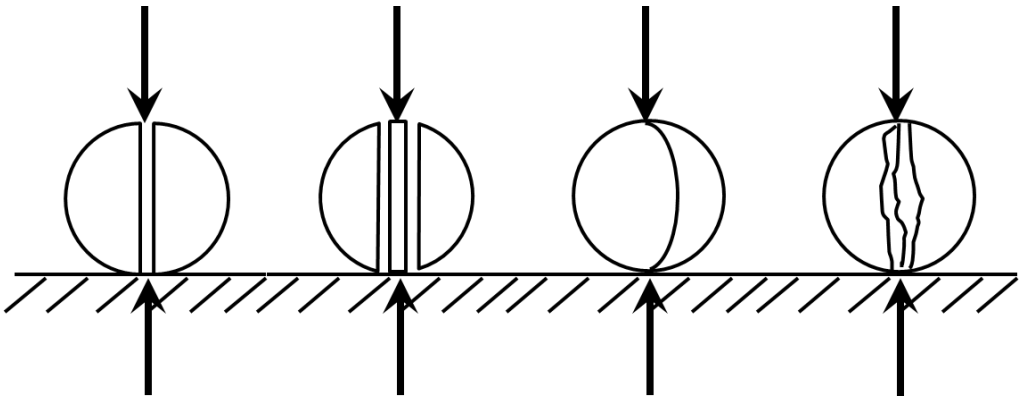

Figure **3-5**: Generalized Mode I fracture orientations. A) Vertical Mode I resulting in two "half moons." B) Branched two strand Mode I fracture with "Island." C) Off-vertical Mode I. D) Multi strand vertical Mode I.

Figure **3-5A**: Example of ideal "half moon" Mode I fracture. Sample 96A.

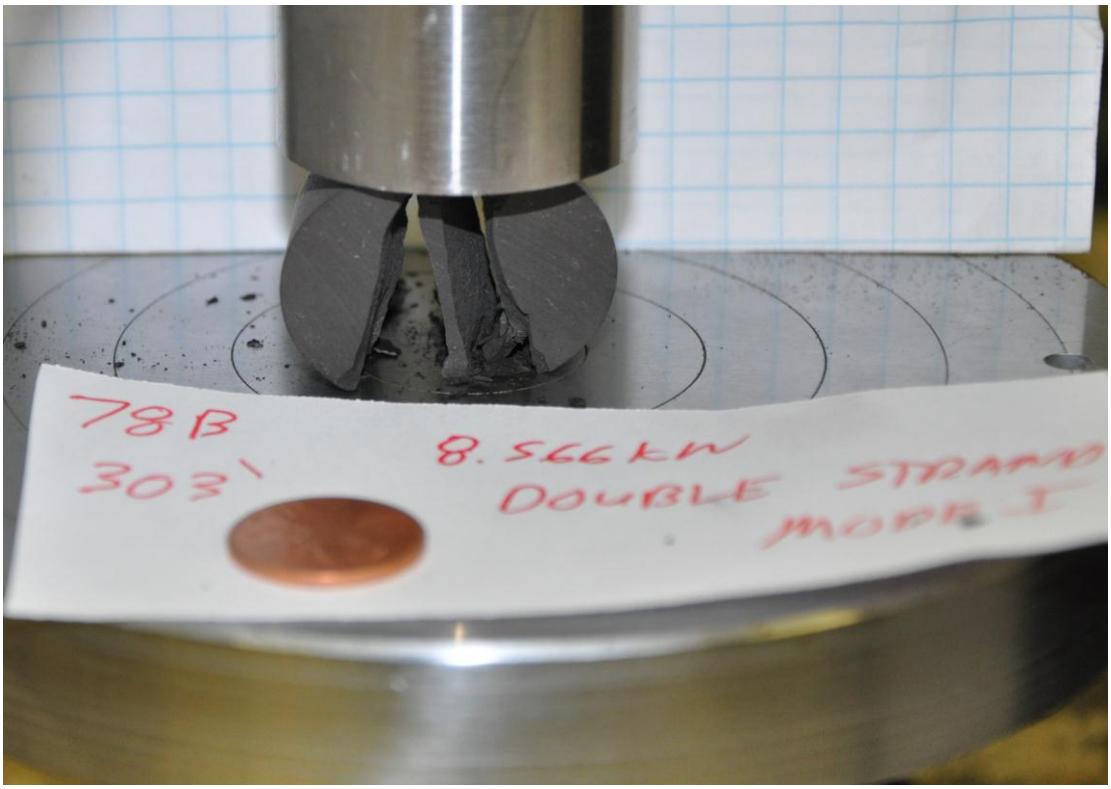

Figure **3-5B**: Example of Branched two strand Mode I fracture with "Island.". Sample 78B.

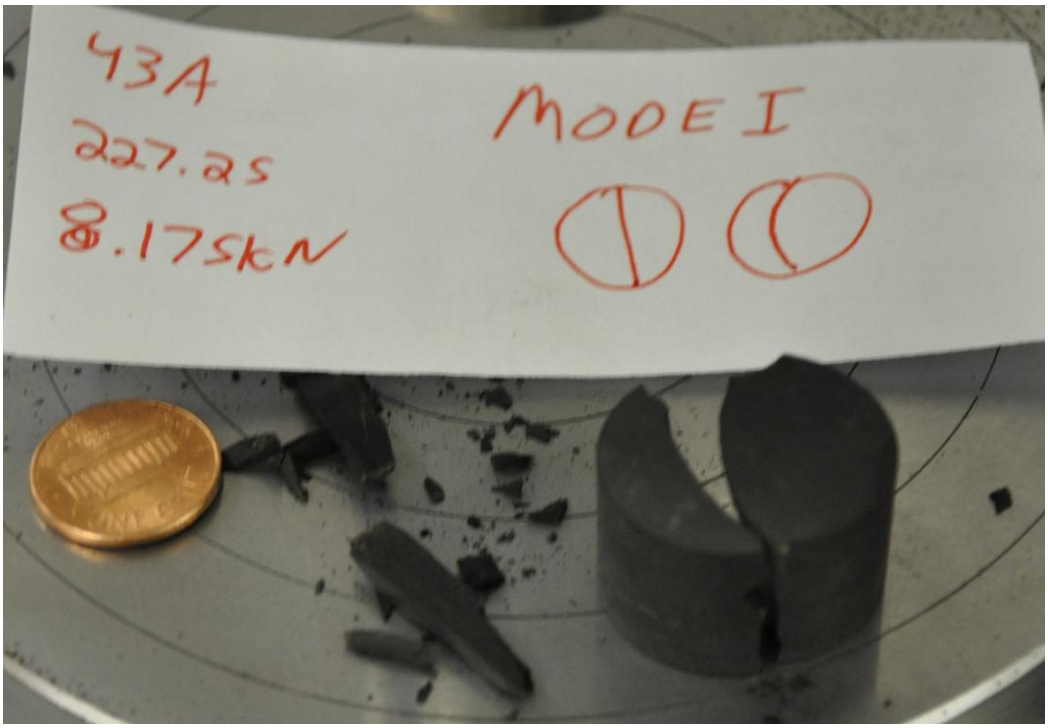

Figure **3-5C**: Example of "Off-vertical Mode I" failure. Sample 43A.

Figure **3-5D**: Example of "Off-vertical Mode I" failure. Sample 96B.

B. Spurious Fractures

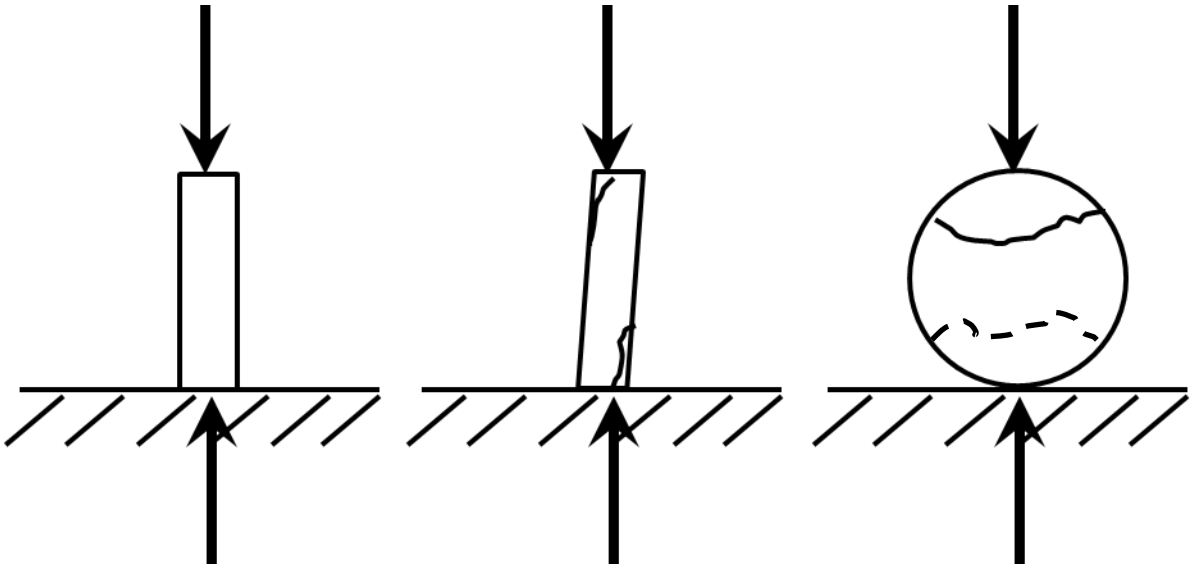

Figure **3-6a**: Depiction of "Roll-over Tilt Collapse" where thin disks fail along bedding on edges due to deformation during loading due to stress concentration on edges when either the disk faces are not perpendicular to the bearing block or the beds not parallel to the disk face.

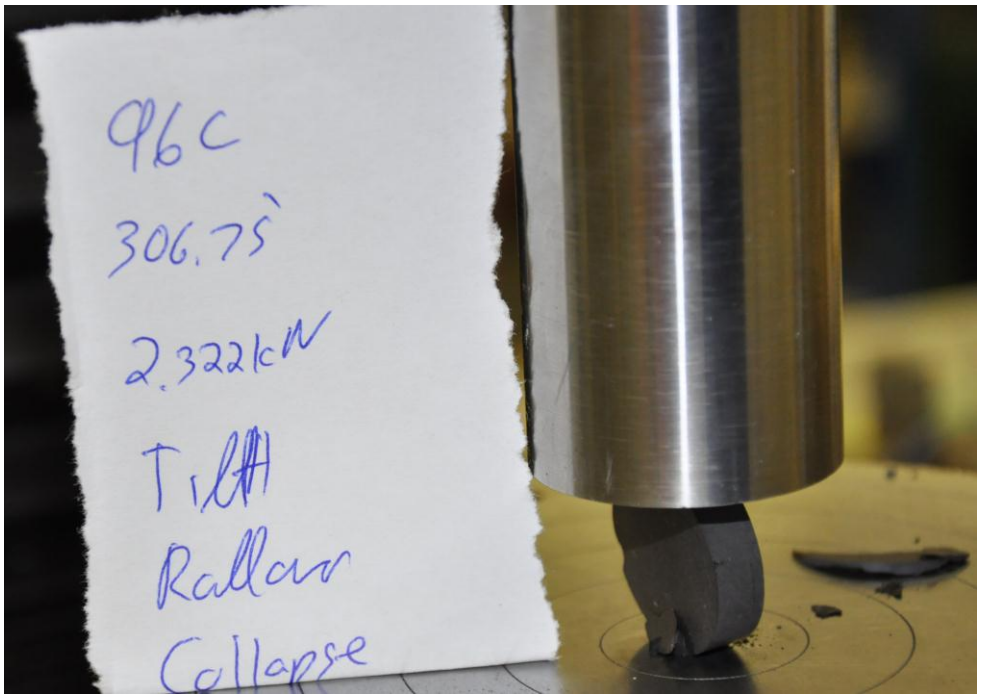

Figure **3-6b**: Example of "Roll-over Tilt Collapse" failure. Sample 96C.

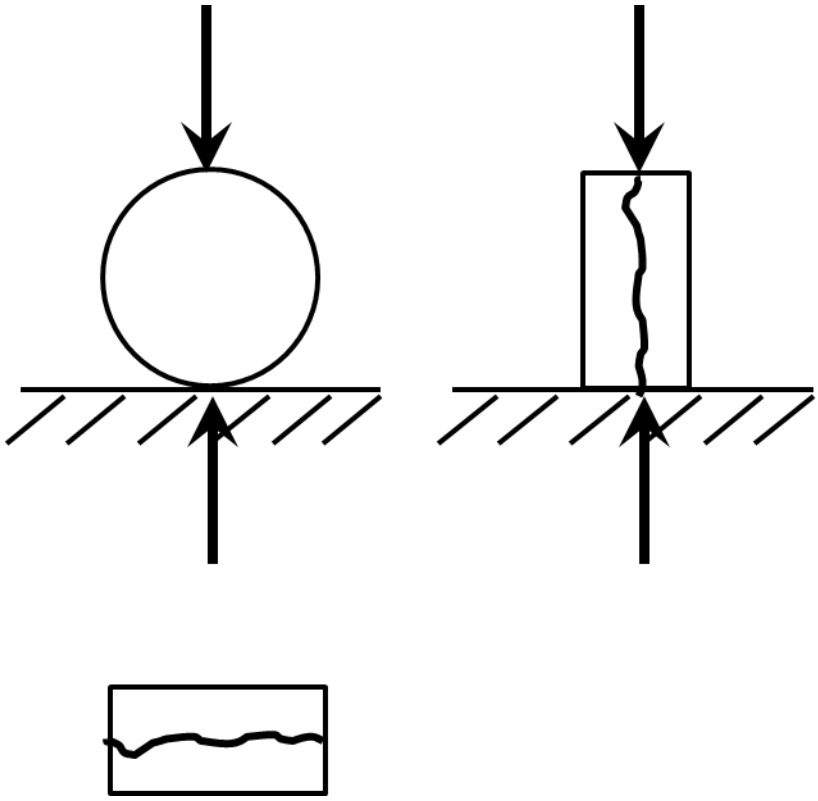

Figure **3-7a**: Front, side, and top view of single strand failure along bedding.

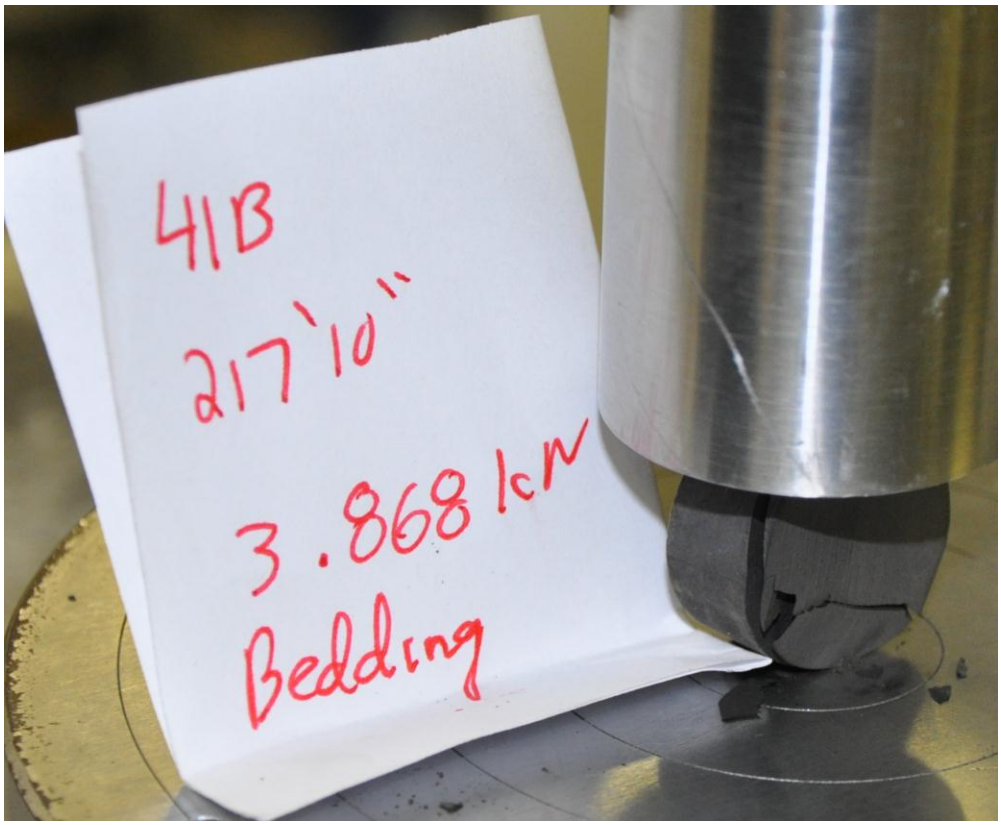

Figure **3-7b**: Example of failure along bedding. Sample 41B.

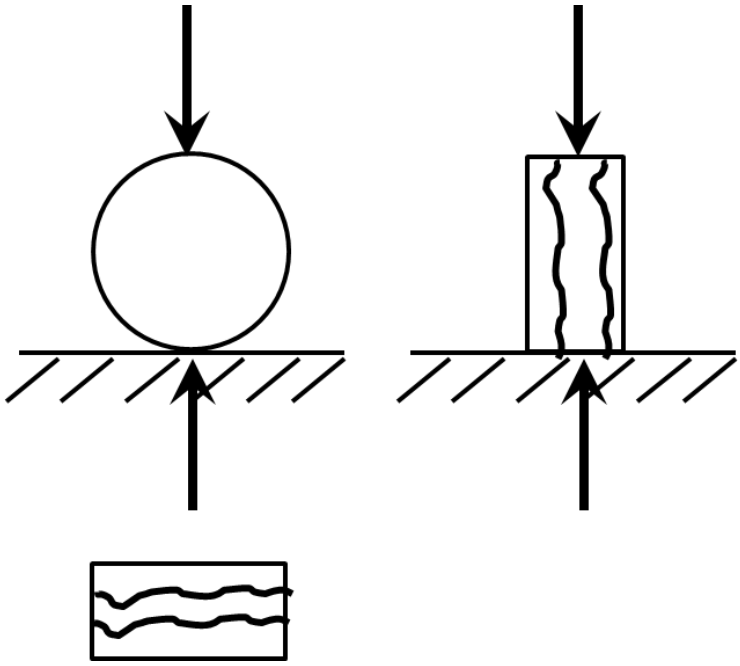

Figure **3-8a**: Front, side, and top view of multiple failures along bedding.

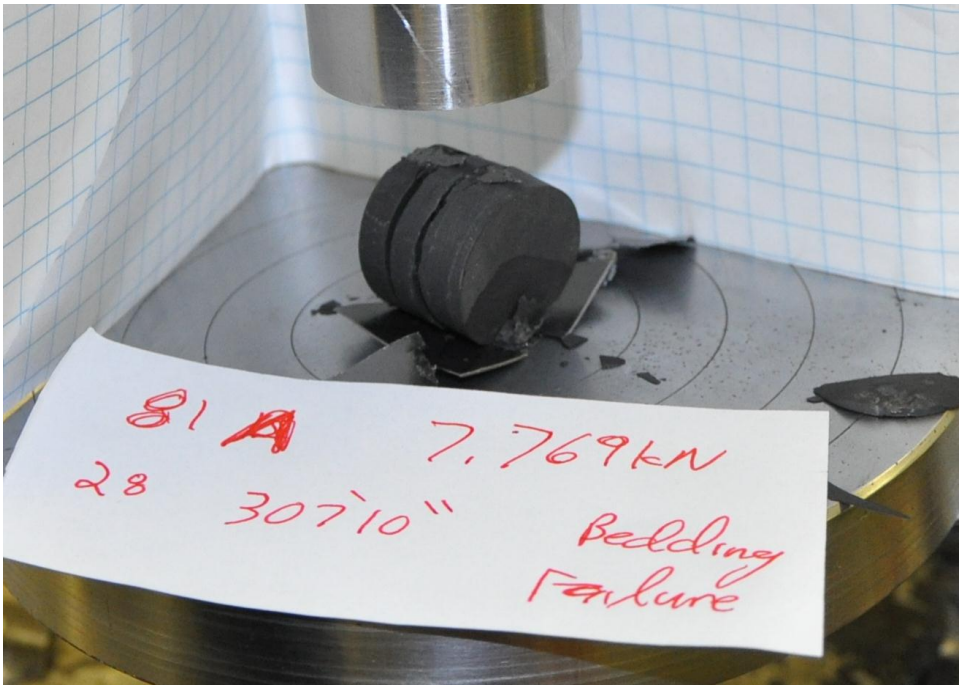

Figure **3-8b**: Example of multiple failures along bedding. Sample 81A.

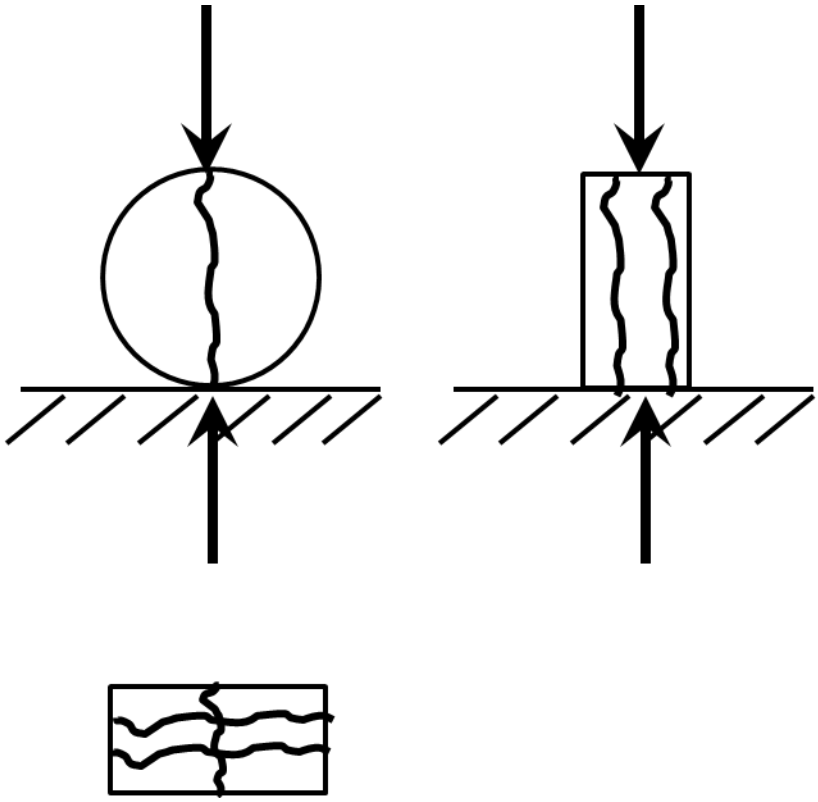

Figure **3-9a**: Front, side, and top view of complex Mode I failure both along bedding and vertically through bedding.

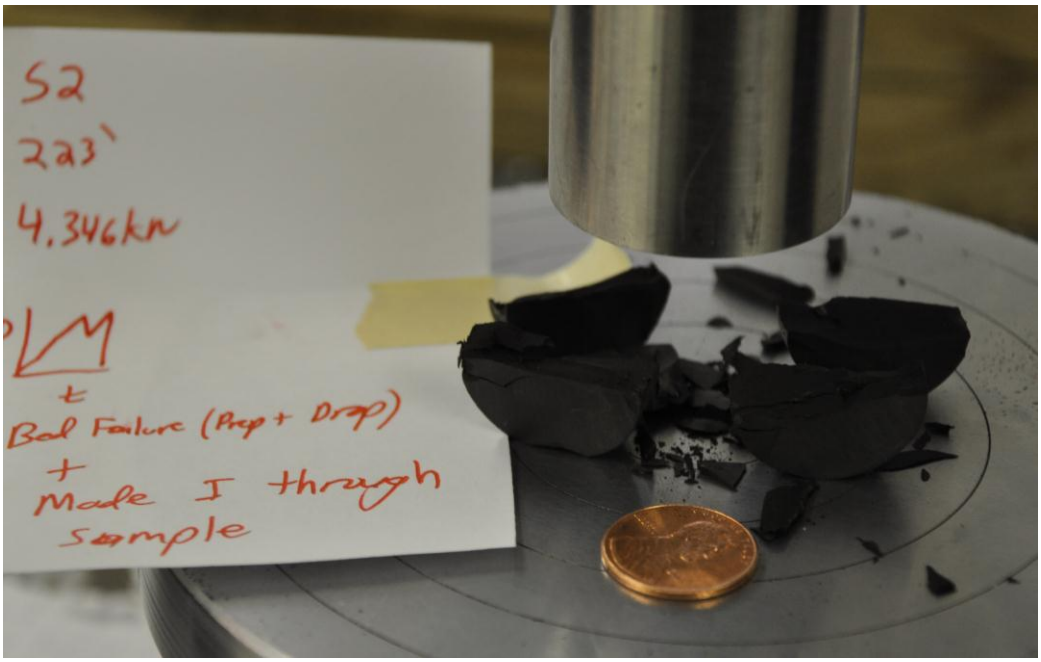

Figure **3-9a**: Example of complex Mode I failure and bedding failures. Sample 52.

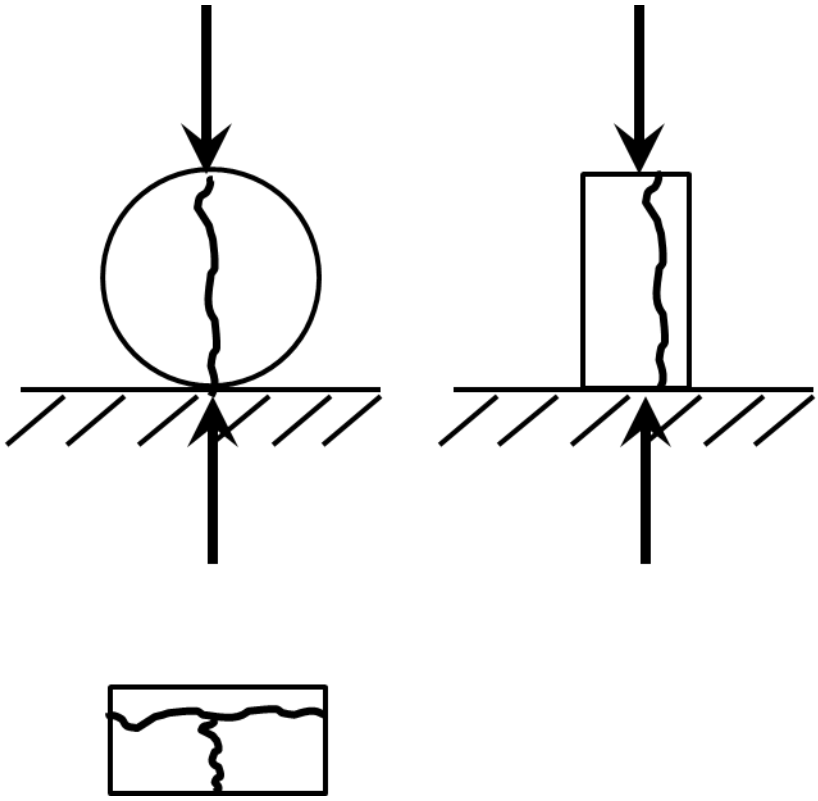

Figure **3-10a**: Front, side, and top view of complex failure along bedding with non-fully penetrating vertical Mode I fracture terminating on bedding failure.

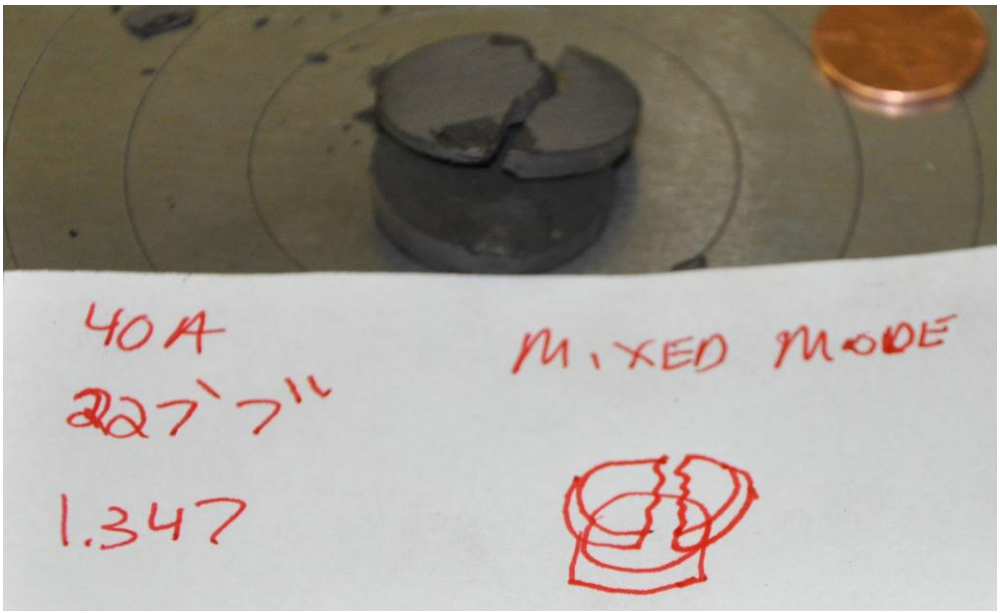

Figure **3-10b**: Example of complex non fully penetrating vertical Mode I fracture terminating on bedding failure. Sample 40A.

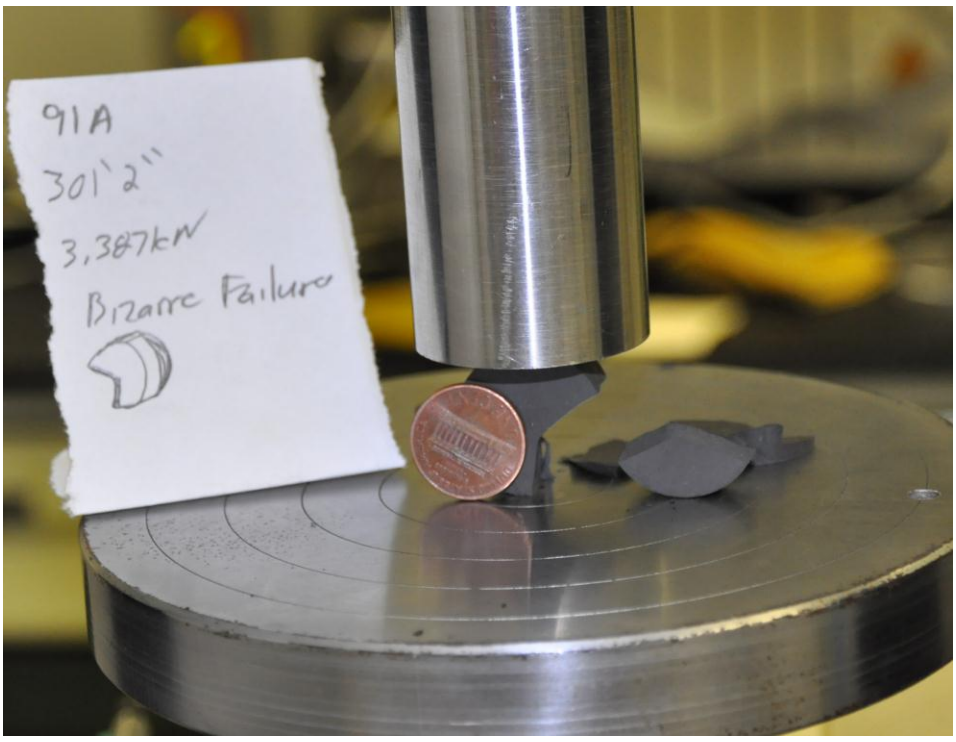

Figure **3-11**: Example of spurious fracture orientation where one third of sample failed. Sample 91A.

Chapter 4

Discussion

1. Experimental Confidence and Influence of Sample Preparation

The pooled sample loading curves (kN) vs time (sec) (Fig 3-1a,b) and (kN) vs dimensionless sample geometry (Fig 3-3a) combined with observations of resulting fractures (Fig 3-5A) produced during Brazilian testing indicate that the experimental results of qualifying samples can be taken as reliable since the desired Mode I fracture orientation cutting across bedding was achieved, peak load required to initiate fracture increased with disk thickness, and the lithologies tested behaved as brittle materials with well-defined stress drops indicating that fracture has occurred. While there were spurious fracture orientations observed due to limitations in sample preparation, 36 samples out of 82 total tested were suitable for use in comparing the tensile strength of calcareous gray shale and the shaley limestone.

The primary difficulty in preparing samples was trying to re-drill sample cores perpendicular to bedding and to polish the disk faces perpendicular to the disk axis. The intention was to minimize transverse isotropic effects due to bedding by orienting bedding parallel to the disk face to ensure that Mode I fractures would propagate through beds and not along them. Thin samples were particularly vulnerable and would tilt over or fail along bedding when not properly prepared. In addition, firm control of the Brazilian disk diameter was limited due to whirling of the core barrel during acquisition. The consequence of this whirling is that thicker samples (larger L/D ratios) tended to experience more problems with “hour glassing” where only a small linear portion of the core would be supporting the disk during loading, resulting in elevated stresses in the core that promoted failure along bedding. Steps were taken during testing to

maximize disk contact with the bearing plates (minimize hour glassing), but due to limited resources it was not possible to entirely eliminate this situation.

"Hour glassing" and bedding dip ($\theta > \sim 2^{o}$) are offered as explanation for the strength fall off observed in Figure 3-3a above dimensionless geometry ratio of 0.7. At these thicknesses, the length of intact core increases, and subsequently the potential for hour glassing. When the Brazilian tests are filtered to reject non-Mode I failures (Fig 3-4a) , the amount of noise is reduced and two important observations can be made. The first observation is that loading rate (strain rate) does not appreciably impact calculated tensile strength. The second observation is that linear trends become apparent in both lithologies. The strong linear trend in peak load (kN) vs dimensionless geometry between 0.3 and 0.7 for the shaley limestone and the calcareous gray shale are taken to be indicative of the selectivity of thin samples with respect to disk preparation, in particular bedding dip with respect to the grid face. Thin disks are not as susceptible to hour glass effects, so if they do not fail immediately along bedding they are likely to be of higher quality than thicker samples that can mask preparation problems and under-report tensile strength since a sub maximal load will cause the sample to fail.

2. Comparison of Lithology Tensile Strength

From the filtered Mode I data (Table 3-1, Fig 3-4a-d), the shaley limestone appears marginally stronger than the calcareous gray shale because the upper most peak load (kN) vs dimensionless sample size for the shaley limestone is slightly higher. In addition, the converted tensile strength (normalization of peak load and sample size), the shaley limestone is again slightly larger. From this pool, the average tensile strengths and standard deviations are 11.14 / 2.15 MPa and 11.07/1.45 MPa respectively. This difference of 0.07 MPa when inserted into Hubbert and Willis' relation (Hubbert and Willis, 1957) would change the fracture pressure < 14 psi, and is therefore insignificant. However, it is apparent that there is a bimodal distribution in tensile strength in the shaley limestone, while there is a more uniform distribution in the calcareous gray shale. Examination of the applicable portions of the gamma ray logs for these wells show the high degree of heterogeneity in the formation compared to the less variable calcareous gray shale log appearance (Fig 2-2a,b). In Figure 3-4c, there is an anomalous group of three shaley limestone samples that are apart from the principal trend line. These samples all came from the same depth (308') which corresponded to a low API gamma ray interval, so this change in lithology likely changed the mechanical properties.

Chapter 5

Conclusion

The Brazilian Disk test was successfully used to determine the Mode I tensile strength of two lithologies (calcareous gray shale and a shaley limestone) in the upper portion of the Oatka Creek Member of the Marcellus Shale. determination in strongly transversely isotropic materials is possible, although care must be taken to ensure that bedding is as parallel as possible to the disk face. It is recommended that similar studies undertaken in shales be conducted in the same fashion (drilling perpendicular to bedding), to both reduce the negative effects of transverse isotropy (failure along bedding rather than across bedding), and to reduce the cost and difficulty of disk preparation. It is further recommended that ASTM D -3967 suggested procedures be modified to only use samples with dimensionless thickness to diameter ratios less than 0.7 due to difficulty in obtaining consistent results and the high selectivity of thinner samples to produce the desired fracture orientation or quickly fail in an obviously spurious fashion. The objective of this study was to compare the tensile strength of the lithologies in question (shaley limestone and calcareous gray shale), and while the absolute difference was small (11.14 MPa vs. 11.07 MPa), the importance of a well constrained stratigraphic framework which to assemble a predictive geomechanical model cannot be understated. To expand the utility of this study, it is recommended that future investigators follow the protocol of Abou-Sayed and Brechtel (1978) and validate laboratory determined values for tensile strength of these lithologies using field hydraulic fracturing data.

Chapter 6

References

Abou-Sayed, A. S., and C. E. Brechtel, 1978. In situ stress determination by hydrofracturing: a fracture mechanics approach, Journal of Geophysical Research, v. 83, no. B6, p. 2851-2862.

Al-Shayea, N. A., K. Khan, and A. Abduraheem, 2001. Fracture toughness vs. tensile strength for reservoir rocks from Saudia Arabia, ISRM sponsored International– 2nd Asian Rock Mechanics Symposium, Beijing, China, September, pp. 169 - 172.

ASTM., 2008. Standard Test Method for Splitting Tensile Strength of Intact Rock Core Specimens, American Society of Testing Materials International, Designation 3967.

Ayatollahi, M. R., and M. R. M. Aliha, 2008. On the use of Brazilian disc specimen for calculating mixed mode I-II fracture toughness of rock materials, Engineering Fracture Mechanics, v. 75, p. 4631-4641.

Bureau of Topographic and Geologic Survey, 2007, Geologic Map of Pennsylvania: Department of Conservation and Natural Resources (DCNR) Map 7, scale 1:2,000,000, http://www.dcnr.state.pa.us/topogeo/maps/map7.pdf, (accessed Feb 24th, 2011).

Chang, S., C. Lee, S. Jeon, 2002, Measurement of rock fracture toughness under modes I and II and mixed-mode conditions by using disc-type specimens, Engineering Geology, v. 66, p. 79-97.

Chen, C., E. Pan, and B. Amadei, 1998. Determination of deformability and tensile strength of anisotropic rock using Brazilian tests, International Journal of Rock Mechanics and Mining Sciences, v. 35, no. 1, p. 43-61.

Claesson, J., and B. Bohloli, 2002. Brazilian test: stress field and tensile strength of anisotropic rocks using an analytical solution, International Journal of Rock Mechanics and Mining Sciences, v. 39, p. 991-1004.

Engelder, T., 1987. Joints and some fractures in rocks, *in* Atkinson, B. K., ed., Fracture Mechanics of Rocks, Academic Press, 27-69.

Guo, H., N. I. Aziz, and L. C. Schmidt, 1993. Rock fracture-toughness determination by the Brazilian test, Engineering Geology, v. 33, p. 177-188.

Haimson, B., and C. Fairhurst, 1967. Initation and extension of hydraulic fractures in rocks, Society of Petroleum Engineers Journal, v. 7, p. 310-318.

Hondros, G., 1959. The evaluation of poisson's ratio and the modulus materials of a low tensile resistance by the Brazilian (indirect tensile) test with particular reference to concrete, Australian Journal of Applied Science, v. 10, no. 3, p. 243-268.

Hubbert, M. K., and B. G. Willis, 1957. Mechanics of hydraulic fracturing, Transactions of the American Institute of Mining, Metallurgical, and Petroleum Engineers, v. 210, p. 153-166.

Lash, G., and T. Engelder, 2011. Thickness trends and sequence stratigraphy of the Middle Devonian Marcellus Formation, Appalachian Basin: Implications for Acadian foreland basin evolution, American Association of Petroleum Geologists Bulletin, v. 95, no. 1, p. 61-103.

Li, L., and M. Aubertin, 2002. A crack-induced stress approach to describe the tensile strength of transversely isotropic rocks, Canadian Geotechnical Journal, v. 39, p. 1-13.

Raleigh, C. B., J. H. Healy, and J. D. Bredehoeft, 1972. Faulting and crustal stress at Rangely, Colorado, *in* Heard, H. C., et al., eds., Flow and Fracture of Rocks, Geophysics Monograph Series, vol. 16, Washington, D.C., American Geophysical Union, p. 275.

Wang, Q. Z., X. M. Jia, S. Q. Kou, Z. X. Zhang, and P. –A. Lindqvist, 2004. The flattened Brazilian disc specimen used for testing elastic modulus, tensile strength and fracture toughness of brittle rocks : analytical and numerical results, International Journal of Rock Mechanics and Mining Sciences, v. 41, p. 245-253.

Appendix A

Laboratory Equipment

INSTRON 4202 RT Loading Apparatus

Appendix B

Brazilian Disk Testing Data Table

This section includes the data collection and results table for all samples tested. It includes sampling depth, sample dimensions (thickness and diameter), lithology, strain rate (mm/min), peak load (kN), calculated tensile stress (MPa), and additional notes on the fracture orientation and mode. It is also available electronically by request from the Appalachian Basin Sequence Stratigraphy Group (ABSSG).

Fracture Results Code:

I = Ideal Vertical Fracture
O = Other Fracture Orientation
M = Mixed Mode Fracture (Vertical Fracture and Fracture Along Bedding)
FB = Failed Along Bedding
T = Sample Tilt or Collapse

Lithology Code:

CGSh = Calcareous Gray Shale w/ Sand

ShLS = Shaley Limestone

Strain Rate High = 1.0mm/min Low =0.500mm/min	Sample Group	Run #	Sample Group Depth (ft KB)	Core Box Number	Diameter (mm)			Average Diameter, D (mm)	Thickness, L (mm)			Average Thickness (mm)	L / D Ratio	Peak Load (kN)	Tensile Strength (Mpa)	Results: (I, M, FB, T)	θ (Degrees)	Comments	Lubrication of Sample	Other Notes	Lithology (Courtesy of Dan Kohl)
Low	44	1	210.75	18	24.78	24.83	24.89	24.83	11.45	11.52	11.51	11.49	0.46	5.17	11.53	I		Perfect complete Mode I.	No Graphite		CGSh
Low	44	2	210.75	18	24.75	24.71	24.80	24.75	9.87	9.82	9.79	9.83	0.40	3.47	9.08	I		Mode I microcrack at loading tip, then sudden Mode I.	No Graphite		CGSh
Low	50	1	212.75	18	24.76	24.86	24.74	24.79	15.93	15.90	15.90	15.91	0.64	3.472	5.60	M		Multiple bed failure, internal Mode I	No graphite		CGSh
Low	50	2	212.75	18	24.73	24.99	24.98	24.99	13.08	13.14	13.07	13.10	0.52	5.197	10.11	FB		Multiple bed failure at peak load.	Graphite		CGSh
Low	45	2	212.833	18	24.72	24.66	24.74	24.71	19.50	19.71	19.77	19.66	0.80	0.4022	0.53	FB		Conchoidal Failure on Bedding, immediately upon start of loading.	No Graphite		CGSh
Low	45	1	212.917	18	24.75	24.77	24.80	24.77	18.58	18.67	18.65	18.63	0.75	6.811	9.39	FB, O		Two small early cracks on bedding during loading, then large release at peak. Large deflection in bearing block observed.	Graphite		CGSh
Low	1	1	217.5	19	24.68	24.54	24.60	24.61	14.85	15.08	15.11	15.01	0.61	6.988	12.04	I		Fracture does not penetrate entire core, but is vertically oriented.			CGSh
Low	1	2	217.5	19	24.66	24.63	24.67	24.65	8.44	8.31	8.43	8.39	0.34	2.854	8.78	O , M		Premature non-vertical fracture, some failure across bedding			CGSh
Low	1	3	217.5	19	24.56	24.57	24.76	24.63	6.53	6.44	6.19	6.39	0.26	1.582	6.40	T		Sample titled over and failed			CGSh
Low	40	0	217.833	19	24.69	24.78	24.75	24.74	16.64	16.64	16.53	16.60	0.67	9.302	14.42	I		Catastrophic Mode I. Two strand failure.	No Graphite		CGSh
High	41	1	217.833	28	24.67	24.70	24.65	24.67	15.60	15.80	15.58	15.66	0.63	7.775	12.81	I		Multi strand Mode I.	No Graphite		CGSh
High	41	2	217.833	28	24.76	24.81	24.78	24.78	10.37	10.35	10.34	10.35	0.42	3.868	9.60	FB		Bedding Failure.	No Graphite		CGSh
Low	53	1	218	19	24.84	24.70	24.71	24.75	12.30	12.00	12.48	12.26	0.50	4.224	8.86	I		Small vertical fracture started at load block, then propogated mode I	No Graphite		CGSh
Low	53	2	218	19	24.63	24.57	24.60	24.60	9.22	9.31	9.28	9.27	0.38	1.42	3.96	O		Exploited weak spot, off center Mode I	No Graphite	slightly off center and wobbly core.	CGSh
Low	51	1	218.25	19	24.71	24.75	24.74	24.73	20.40	20.32	20.38	20.37	0.82	4.881	6.17	M		Combination early bedding fail, late Mode I on some beds. Heavy disection of core along bedding.	Graphite	Ball Bearing Bearing Surface.	CGSh
High	52	1	223	20	24.61	24.73	24.72	24.69	16.67	16.74	16.64	16.68	0.68	4.346	6.72	I, M		Bed failure propagated at 0.4kN, Bedding failure, then rebuild to Mode I though entire sample	No Graphite		CGSh

Low	21	1	225.75	20	24.84	24.63	24.66	24.71	9.58	9.93	9.96	9.82	0.40	2.332	6.12	FB		Failed along bedding.			CGSh
Low	43	1	227.25	20	24.70	24.75	24.77	24.74	16.92	16.97	16.82	16.90	0.68	8.175	12.45	I		Mode I Failure	No Graphite		CGSh
Low	43	2	227.25	20	24.80	24.79	24.82	24.80	7.56	7.53	7.52	7.54	0.30	3.013	10.26	I		Mode I Failure.	No Graphite		CGSh
High	42	1	227.5	21	24.63	24.65	24.69	24.66	16.48	16.53	16.20	16.40	0.67	5.85	9.21	I, M		Mode I, plus internal bed fail. Mode I did not propagate through entire sample.	No Graphite		CGSh
Low	40	1	227.583	20	24.87	24.76	24.76	24.80	6.50	6.53	6.49	6.51	0.26	1.347	5.31	M		At 1kN, front bedding failure followed by Mode I failure at peak on other bed.	No Graphite		CGSh
Low	40	2	227.583	20	24.72	24.73	24.73	24.73	12.68	12.64	12.62	12.65	0.51	5.095	10.37	I		Two strand perfect Mode I.	No Graphite		CGSh
Low	40	3	227.583	20	24.74	24.72	24.70	24.72	9.05	9.03	9.02	9.03	0.37	2.295	6.54	FB		Bedding failure.	No Graphite		CGSh
High	46	1	229.5	20	24.72	24.76	24.88	24.79	14.67	14.61	14.48	14.59	0.59	5.97	10.51	I		Catastrophic Mode I	No Graphite		CGSh
Low	39	1	229.667	20	24.71	24.77	24.82	24.80	18.68	18.54	18.76	18.66	0.75	4.961	6.83	I		Mode I through core, then bedding failures.	No Graphite		CGSh
High	39	2	229.667	20	24.67	24.71	24.54	24.64	14.29	14.45	14.37	14.37	0.58	6.226	11.19	M		Bedding failure, with internal Mode I	No Graphite		CGSh
Low	38	2	229.75	20	24.97	24.71	24.79	24.82	17.92	17.94	17.96	17.94	0.72	8.564	12.24	I		Mode I, two strand failure. Internal bisection along beds.	No Graphite		CGSh
High	38	1	229.917	20	24.69	24.82	24.78	24.76	14.73	14.44	14.18	14.45	0.58	5.992	10.66	I		Catastrophic Mode I	No Graphite		CGSh
High	37	1	230	21	24.65	24.62	24.53	24.60	17.58	17.56	17.74	17.63	0.72	7.168	10.52	I		Small bed crack at 2kN, bed failure, then Mode I at peak.	No Graphite		CGSh
Low	48	1	231.5	20	24.67	24.77	24.77	24.74	12.99	12.98	12.95	12.97	0.52	2.748	5.45	FB		Sudden failure on bedding.	No Graphite		CGSh
Low	31	1	232.167	21	24.72	24.78	24.75	24.75	17.71	17.76	17.84	17.77	0.72	7.581	10.97	I		Perfect Mode I.	No graphite		CGSh
Low	33	1	232.833	21	25.23	24.71	24.73	24.89	19.21	19.03	19.05	19.10	0.77	4.224	5.66	FB		Multiple failures along bedding	Graphite		CGSh
High	33	2	232.833	21	24.75	24.67	24.70	24.71	19.09	19.14	19.05	19.09	0.77	6.381	8.61	M		Shallow Mode I, multiple fractures on Bedding	Graphite		ShLS
Low	32	2	233	21	24.81	24.75	24.75	24.77	17.17	17.17	17.24	17.19	0.69	5.264	7.87	I		Mode I microcrack at 4.5kN, then one dominant strand Mode I faiure at peak load.	No Graphite		CGSh
Low	32	1	233	21	24.80	24.76	24.75	24.77	12.19	12.16	12.25	12.20	0.49	4.843	10.20	I, M		Mixed Mode bending Vertical Mode I fracture. Vertical in center on front, curved on edge in back.	No Graphite		CGSh

Low	32	3	233	21	24.77	24.74	24.74	24.75	13.52	13.36	13.58	13.49	0.54	5.723	10.92	I		Small bedding microcrack before Mode I	No Graphite		CGSh
High	3	3	235.25	21	24.75	25.19	24.74	24.89	16.79	16.84	16.79	16.81	0.68	4.843	7.37	M		Multiple Bedding Failures, Internal Mode I	Graphite		CGSh
High	3	2	235.375	21	24.80	24.78	24.86	24.81	19.19	18.86	19.49	19.18	0.77	7.522	10.06	FB		Very Early Bedding Break ~0.4kN	Graphite		CGSh
High	3	1	235.5	21	24.78	24.79	24.59	24.72	19.04	19.06	19.06	19.05	0.77	7.026	9.50	M		Extensive Bedding Faults, Internal Mode I?	Graphite		CGSh
High	34	2	236	21	24.73	24.70	24.72	24.72	11.19	11.21	11.39	11.26	0.46	5.103	11.67	FB		Multiple conchoidal/ high angle failures on bedding	Graphite		CGSh
High	34	1	236	21				24.72	19.29	19.35	19.24	19.29	0.78	8.341	11.14	FB		Primary failure on bedding at 8.341kN	Graphite	Used Average Thickness of Same Sample Depth.	CGSh
Low	35	2	236.167	21	24.65	24.73	24.72	24.70	7.20	7.19	7.20	7.20	0.29	2.423	8.68	FB		Bedding Fail	No Graphite		CGSh
Low	35	1	236.167	22	24.71	24.78	24.73	24.74	14.35	14.08	14.45	14.29	0.58	5.35	9.63	I, M		Bedding fail and front with internal Mode I cutting from rear face to front bed.	No Graphite		CGSh
Low	36	1	236.333	21	24.77	24.72	24.70	24.73	14.40	14.40	14.41	14.40	0.58	5.901	10.55	FB		Bedding Fail	No graphite		CGSh
Low	36	2	236.333	21	24.68	24.76	24.79	24.74	17.21	17.27	17.32	17.27	0.70	5.901	8.79	T, FB		Progressive bed and tilt failure.	No graphite		CGSh
Low	2	1	297.5	27	24.74	24.73	24.73	24.73	10.86	10.92	10.76	10.85	0.44	4.843	11.49	T , FB		Sample loaded edge crush and failure along bedding.			ShLS
High	84	1	300.25	28	24.69	24.71	24.73	24.71	19.34	19.05	19.01	19.13	0.77	8.824	11.88	I		Mode I with multiple vertical strands.	No Graphite		ShLS
Low	85	1	300.5	28	24.97	24.78	24.68	24.81	14.65	14.60	14.56	14.60	0.59	5.97	10.49	FB		Multiple bedding failure.	No Graphite		
High	77	1	300.833	28	24.78	24.82	24.73	24.78	18.50	18.51	18.48	18.50	0.75	6.65	9.24	I, M		Mode I, plus some internal bed failure.	No Graphite		ShLS
High	77	2	300.833	28	24.64	24.65	24.69	24.66	19.45	19.20	19.34	19.33	0.78	5.75	7.68	I, O		Non penetrating Mode I. 7.01mm bed failed Mode I.	No Graphite	Warped bottom and top of disk.	ShLS
Low	75	1	301	28	24.64	24.72	24.61	24.66	18.19	17.98	18.16	18.11	0.73	3.981	5.68	M		Half bedding break to creeping Mode I.	No Graphite	Uneven disk base.	ShLS
High	91	1	301.167	28	24.77	24.73	24.76	24.75	12.82	13.28	12.96	13.02	0.53	3.387	6.69	O		Bizarre orientation (Pac Man type failure (6pm - 9pm) shaped failure block.	No Graphite		ShLS
High	91	2	301.167	28	24.76	24.83	24.77	24.79	6.59	6.46	6.53	6.53	0.26	2.395	9.42	T		Tilt bedding collapse.	No Graphite		ShLS
High	92	1	301.167	28	24.93	24.87	24.73	24.84	14.64	14.67	14.96	14.76	0.59	7.18	12.47	I		Half Moon Mode I.	No Graphite		ShLS

High	90	1	301.3	28	24.67	24.74	24.70	24.70	17.79	17.67	17.55	17.67	0.72	10	14.58	I		Mode I half moon failure with Island.	No Graphite		ShLS
Low	20	1	302.5	28	24.72	24.68	24.68	24.69	17.42	17.65	17.30	17.46	0.71	8.666	12.80	I		Perfect Break, Vertical Fracture Straight Through	Graphite		ShLS
Low	20	2	302.5	28	24.74	24.75	24.87	24.79	20.91	20.90	20.86	20.89	0.84	7.879	9.69	I		Vertical but off-center break. Fracture straight through.	Graphite		ShLS
Low	78	1	303	28	24.69	24.68	24.67	24.68	17.16	17.17	17.11	17.15	0.69	6.883	10.35	I		Mode I Failure			ShLS
Low	78	2	303	28	24.74	24.75	24.72	24.74	18.89	18.75	18.68	18.77	0.76	8.566	11.74	I		Double Strand Mode I			ShLS
Low	78	3	303	28	24.68	24.69	24.70	24.69	9.93	9.89	9.92	9.91	0.40	4.683	12.18	FB		Bedding failure preceded by microcracks			ShLS
High	93	1	303	28	24.73	24.72	24.75	24.73	16.79	17.00	16.73	16.84	0.68	8.37	12.79	I		Mode I with island. One half had bed failure.	No Graphite		ShLS
High	93	2	303	28	24.65	24.71	24.74	24.70	13.56	13.44	13.17	13.39	0.54	6.427	12.37	I		Mode I, w/ two strands. Almost perfect half moon fail.	No Graphite		ShLS
High	79	1	306	28	24.75	24.75	24.78	24.76	19.36	19.42	19.47	19.42	0.78	5.906	7.82	I		Mode I.	No Graphite		ShLS
High	79	2	306	28	24.74	24.77	24.68	24.73	19.24	19.14	19.10	19.16	0.77	5.895	7.92	I		Catastrophic Mode I. No bed failures	No Graphite	White specs on face (calcareous)?	ShLS
High	98	2	306	28	24.76	24.77	24.76	24.76	19.37	19.41	19.79	19.52	0.79	7.7442	10.20	I		Mode I, slightly curved with one half bed failure.	No Graphite		ShLS
High	98	1	306	28	24.79	24.90	24.82	24.84	11.54	11.47	11.38	11.46	0.46	5.632	12.59	I		Perfect Mode I half moon failure.	No Graphite		ShLS
High	98	3	306	28	24.61	24.83	24.92	24.79	11.81	11.95	12.21	11.99	0.48	4.67	10.00	I		Half Moon Mode I.	No Graphite		ShLS
High	94	1	306.167	28	24.67	24.63	24.72	24.67	17.73	17.80	17.98	17.84	0.72	5.799	8.39	I		Complex Migrating Mode I fracture.	No Graphite	NOTE: Picture says "sample 96"	ShLS
High	96	1	306.75	28	24.79	24.78	24.78	24.78	12.36	12.28	12.76	12.47	0.50	5.874	12.10	I		Perfect Mode I half moon failure.	No Graphite		ShLS
High	96	2	306.75	28	24.74	24.87	24.73	24.78	10.57	10.48	10.49	10.51	0.42	4.956	12.11	I		Mode I, multi strand half moon.	No Graphite		ShLS
High	96	3	306.75	28	24.77	24.79	24.81	24.79	6.41	6.35	6.39	6.38	0.26	2.322	9.34	T		Tilting roll over fail (bed failure at opposite load points in direction of tilt).	No Graphite		ShLS
Low	80	1	307.667	28	24.75	24.74	24.75	24.75	18.94	18.85	18.87	18.89	0.76	9.627	13.11	I		Catastrophic Mode I, dual strand.			ShLS
Low	80	2	307.667	28	24.74	24.69	24.68	24.70	13.03	13.12	12.95	13.03	0.53	4.205	8.31	I		Mode I			ShLS
Low	81	1	307.833	28	24.71	24.74	24.79	24.75	19.06	18.95	19.04	19.02	0.77	7.769	10.51	FB		Failed along bedding.	Graphite		ShLS
Low	81	2	307.833	28	24.86	24.73	24.76	24.78	19.11	19.13	19.18	19.14	0.77	7.326	9.83	FB		Failed along bedding.	Graphite		ShLS
High	82	1	308	28	24.71	24.63	24.68	24.67	17.02	17.04	17.05	17.04	0.69	6.36	9.63	I		Branched Mode I	No Graphite		ShLS
High	82	2	308	28	24.69	24.61	24.67	24.66	19.52	19.46	19.43	19.47	0.79	5.031	6.67	I		Mode I, no bed failure	No Graphite		ShLS
High	82	3	308	28	24.63	24.67	24.71	24.67	7.89	7.88	7.81	7.86	0.32	2.532	8.31	I		Clean Mode I	No Graphite		ShLS
High	76	1	308.5	28	24.73	24.75	24.75	24.74	17.25	17.36	16.92	17.18	0.69	6.674	10.00	I		Mode I	No Graphite		ShLS
High	76	2	308.5	28	24.68	24.80	24.74	24.74	13.01	13.03	13.10	13.05	0.53	4.773	9.41	I, O		Offcenter curved Mode I	No Graphite		ShLS
High	97	1	309.75	29	24.77	24.67	24.66	24.70	15.13	14.98	15.09	15.07	0.61	5.659	9.68	I		Mode I	No Graphite		ShLS
High	95	1	309.833	29	24.74	24.77	24.78	24.76	14.41	14.35	14.27	14.34	0.58	6.623	11.87	I		Splitting Mode I (Split Front, Single strand Back).	No Graphite		ShLS

VITA

Michael Cronin

EDUCATION

The Pennsylvania State University, University Park, PA **May 2011**

Schreyer Honors College

Bachelor of Science with Honors in **Geosciences**
Department of Geosciences

Bachelor of Science with Honors in **Petroleum and Natural Gas Engineering**
Department of Energy and Mineral Engineering

RESEARCH INTERESTS

-Geomechanical Modeling in Unconventional Reservoirs

-Multiphase Reservoir Simulation

-Methane Hydrates

-Pore Pressure Prediction

-Wellbore Integrity

RESEARCH & RELEVANT WORK EXPERIENCE

Penn State University, Dept. of Geosciences Oct 2010-May 2011

Undergraduate Thesis Researcher

Advisors: Dr. Terry Engelder (Geosciences)

Project: Calibration of hydraulic fracturing field tests using brazilian disk tests to define tensile strength of two Marcellus Shale lithologies.

Geosciences Outcomes:

-Experience in core sample preparation and measurement of rock tensile strength using Brazilian Disk testing.

PNGE Outcomes:

-Utilize generated Marcellus rock properties and relate to current hydraulic fracturing theory.

ConocoPhillips, Lower 48 E&P May 2010-Aug 2010

Production/Reservoir Engineering Intern

-Researched a shut-in wellbore's history to evaluate mechanical condition and recompletion/remedial options.
-Calculated reserves and restored production potential to assess remedial economics.
-Identified and implemented five artificial lift projects for gas wells.
-Improved technical presentation skills presenting project to mentor team and business unit.

United States Geological Survey, **Menlo Park**, **CA** May 2009-Aug 2009

Student Hydrologist Intern

Advisor: Dr. John R. Nimmo

Project: Using Electrical Resistivity Tomography (ERT) to determine volumetric water content in shallow vadose zone.

Key Outcomes:

-Developed new application of non-traditional dye tracer for use in electrical resistivity imaging.
-Presented formal and informal research and work progress summaries to project team and collaborators.

SELECTED COURSEWORK

Engineering: Reservoir Modeling and Evaluation, Secondary Recovery, Analytical Well Testing (Spring) Drilling, Production, Rock Properties

Geosciences: Structural Geology, Petroleum Geology, Seismology, Sedimentology, Hydrogeology.

Mathematics: Calculus I – III, Linear Algebra, Differential Equations.

TECHNICAL SKILLS

MATLAB, Fekete RTA, CMG, OFM, Snap, ArcGIS, Delft3D, C++, Minitab, Stella, Powerpoint, Excel.

HONORS & AWARDS

Academic:

College of EMS Engineering Honor Graduate 2011

Phi Beta Kappa	2011
PNGE Undergraduate Merit Award	2010
SPE Pittsburgh Petroleum Section Scholarship Winner	2010
Schreyer Honors College Summer Internship Grant	2009
USGS-NAGT Cooperative Field Training Program Intern	2009
Phi Kappa Phi	2008
American Collegiate Rowing Association First Team Academic All American	2008,2009
Marathon Oil Honors Scholarship	2006-2010
Schreyer Honors College Scholar	2006

Leadership:

Eric A Walker Award	2011
USA Today Student Leadership Award	2010
Theta Chi Fraternity Sherwood Blue Scholarship	2009,2010
Omicron Delta Kappa	2009

PROFESSIONAL MEMBERSHIPS

American Institute of Petroleum Geologists	2011
Society of Petroleum Engineers	2009
American Association of Petroleum Geologists	2009

LANGUAGE SKILLS

English: Native speaker.
French: Fluent through 10+ years of study.